

Photon & Pion induced reactions for the study of nucleon resonances

Sang-Ho Kim (金相鎬)

Research Center for Nuclear Physics (RCNP)
Osaka University

In collaboration with

- Atsushi Hosaka (RCNP)
- Hyun-Chul Kim (Inha Univ.& RCNP)
- Hiroyuki Noumi (RCNP)



Outline

$$\pi^- p \rightarrow K^{*0} \Lambda$$

$$\pi^- p \rightarrow D^{*-} \Lambda_c^+$$

$$\gamma p \rightarrow K^{*+} \Lambda$$

- ◆ Motivation
- ◆ Formalism
(Effective Lagrangian & Regge model)
- ◆ Results :
 - total cross sections (σ)
 - differential cross sections
($d\sigma/d\Omega$, $d\sigma/dt$)
 - polarization observables
- ◆ Summary

$$\begin{array}{l} \mathbf{I} \\ \mathbf{\cdot} \end{array} \quad \begin{array}{l} \pi^- p \rightarrow K^{*0} \Lambda \\ \pi^- p \rightarrow D^{*-} \Lambda_c^+ \end{array}$$

Limits on Charm Production in Hadronic Interactions near Threshold

J. H. Christenson, E. Hummel,^(a) G. A. Kreiter, and J. Sculli, P. Yamin
New York University, New York, New York 10003

Brookhaven National Laboratory, Upton, New York 11973

(Received 28 January 1985)

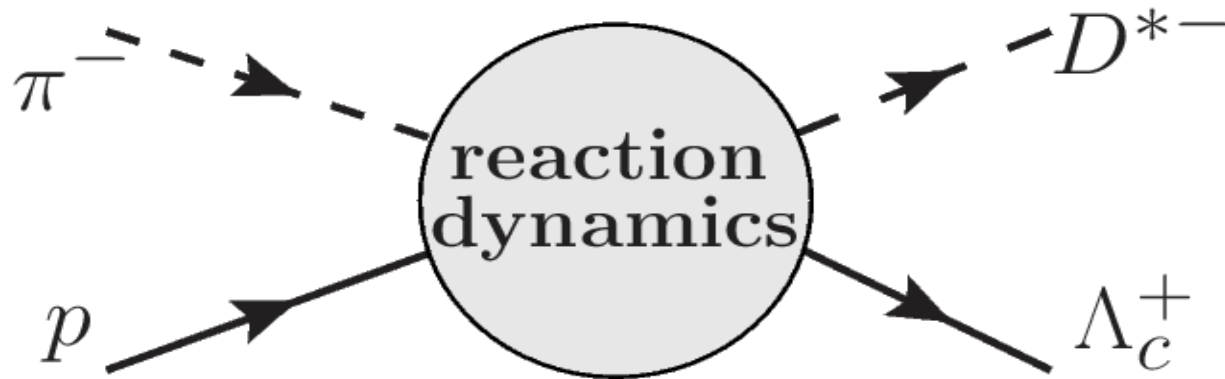
We present the results of an experiment to search for associated charm production near threshold in 13-GeV/c $\pi^- p$ interactions. A large-aperture proportional wire chamber spectrometer was sensitive to the decay fragments of the forward-produced D^{*-} 's expected from the two-body reactions $\pi^- + p \rightarrow D^{*-} + \Lambda_c^+, \Sigma_c^+, \dots$. The missing baryon mass was determined from the vector momenta of the incident pion and the candidate D^{*-} . No evidence for these reactions was found, which resulted in a 7-nb upper limit (95% confidence level) for each of the cross sections $\sigma(\pi^- p \rightarrow D^{*-} \Lambda_c^+)$ and $\sigma(\pi^- p \rightarrow D^{*-} \Sigma_c^+)$.

Proposal P50 is submitted :

December 10, 2012

Executive Summary

We propose the spectroscopic study of charmed baryons via the (π, D^{*-}) reactions at the high-momentum (high-p) beam line of J-PARC to investigate the diquark degree of freedom in a hadron. The good diquark correlation is due to the color-spin interaction whose strength is proportional to the inverse of a quark mass. Therefore, there would be only one good diquark pair in a charmed baryon, which makes the study of excited charmed baryons unique and interesting.



Effective Lagrangian

The contribution of the ground state

Good at describing Low energy(threshold) behavior

Parameters : **coupling constants**, cut off masses in form factors

Regge Model

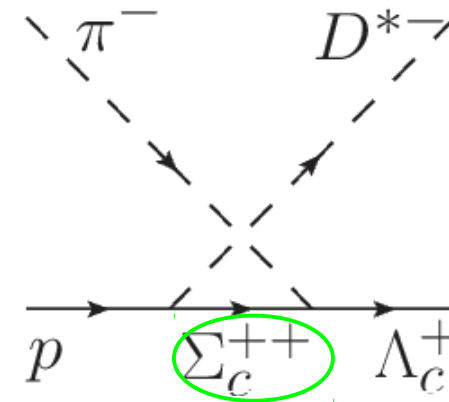
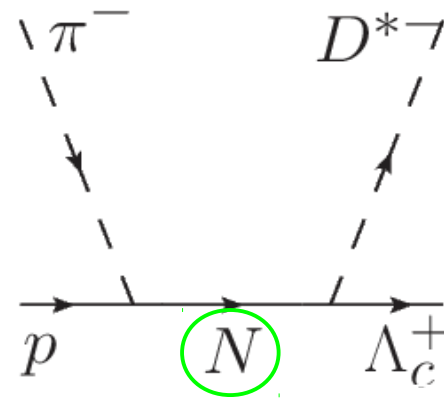
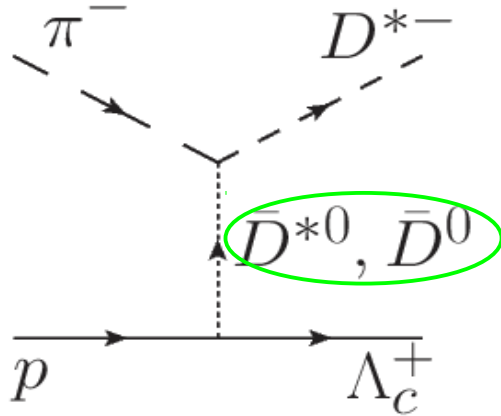
The contribution of both the ground and excited states which lie in the same trajectory

Good at describing High energy behavior

Parameters : **coupling constants**, Regge trajectories, scale parameters

Tree Level Diagrams

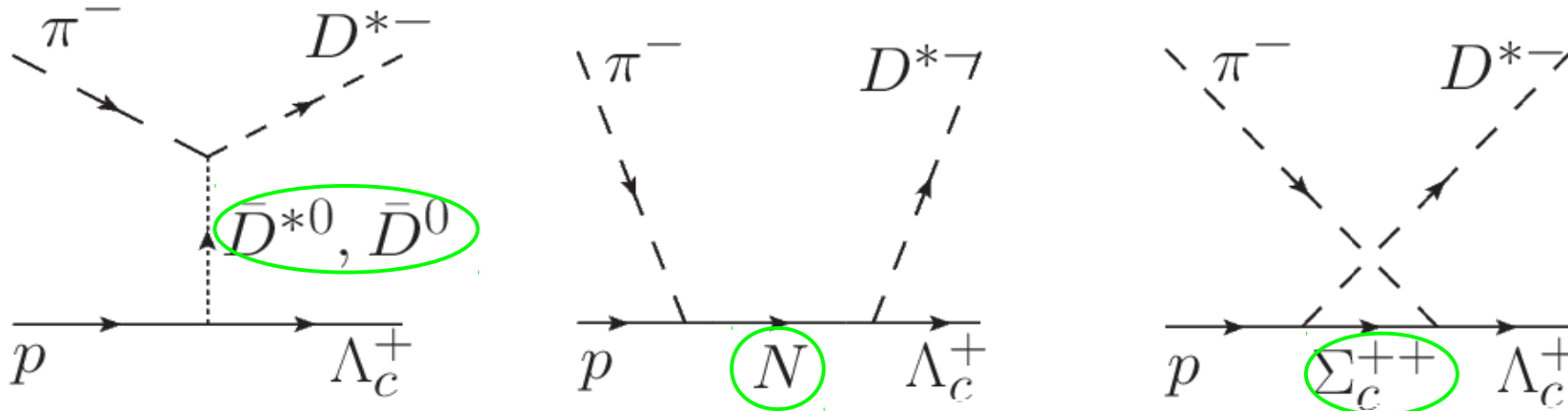
$\pi^- p \rightarrow D^{*-} (2010) \Lambda_c^+ (2286)$



c quark

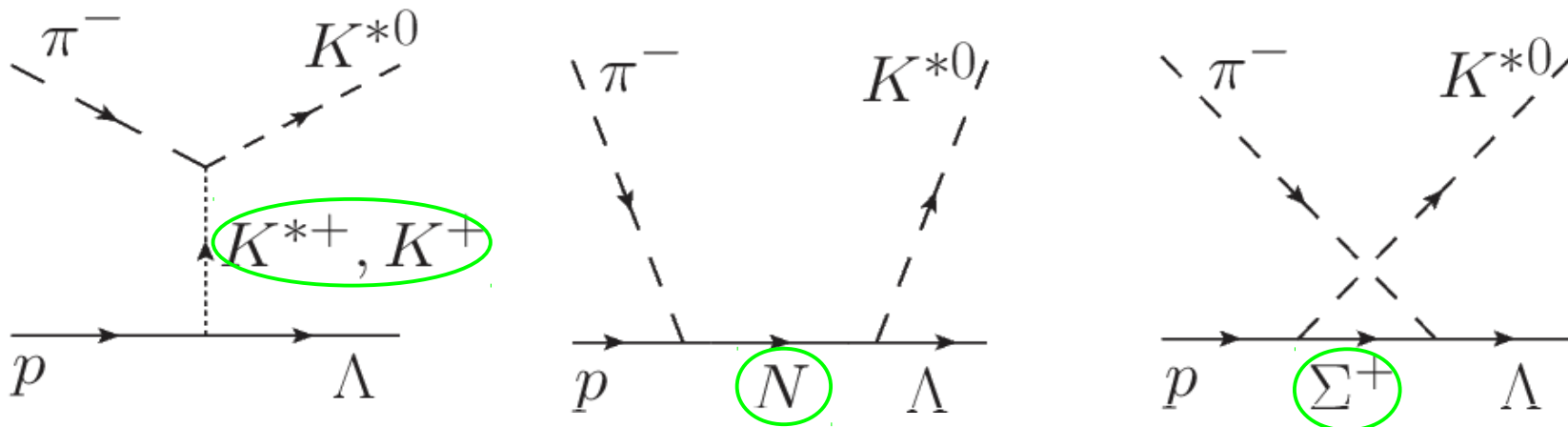
Tree Level Diagrams

$$\pi^- p \rightarrow D^{*-} (2010) \Lambda_c^+ (2286)$$



c quark

$$\pi^- p \rightarrow K^{*0} (892) \Lambda (1116)$$



s quark

The same coupling constants will be used for the corresponding vertices.

Effective Lagrangians

$$\mathcal{L}_{\pi K K^*} = -ig_{\pi K K^*} (\bar{K} \partial^\mu \tau \cdot \pi K_\mu^* - \bar{K}_\mu^* \partial^\mu \tau \cdot \pi K)$$

$$\mathcal{L}_{\pi K^* K^*} = -g_{\pi K^* K^*} \varepsilon^{\mu\nu\alpha\beta} \partial_\mu \bar{K}_\nu^* \tau \cdot \pi \partial_\alpha K_\beta^*$$

$$\mathcal{L}_{\pi N N} = \frac{g_{\pi N N}}{2M_N} \bar{N} \gamma_\mu \gamma_5 \partial^\mu \tau \cdot \pi N,$$

$$\mathcal{L}_{\pi \Sigma \Lambda} = \frac{g_{\pi \Sigma \Lambda}}{M_\Lambda + M_\Sigma} \bar{\Lambda} \gamma_\mu \gamma_5 \partial^\mu \pi \cdot \Sigma + \text{H.c.}$$

$$\mathcal{L}_{K N \Lambda} = \frac{g_{K N \Lambda}}{M_N + M_\Lambda} \bar{N} \gamma_\mu \gamma_5 \Lambda \partial^\mu K + \text{H.c.}$$

$$\mathcal{L}_{K^* N Y} = -g_{K^* N Y} \bar{N} \left[\gamma_\mu Y - \frac{\kappa_{K^* N Y}}{2M_N} \sigma_{\mu\nu} Y \partial^\nu \right] K^{*\mu} + \text{H.c.}$$

Coupling Constants

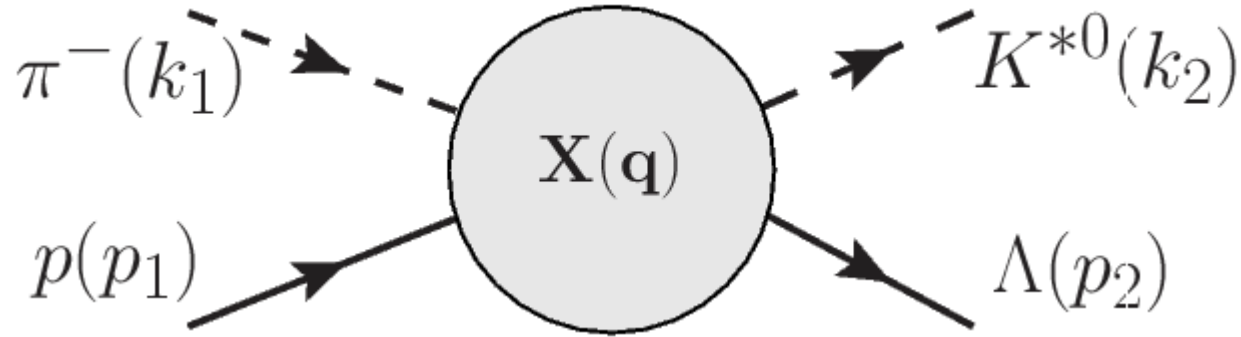
$g_{\pi K K^*}$	$g_{\pi K^* K^*}$	$g_{\pi N N}$	$g_{\pi \Sigma \Lambda}$	$g_{K N \Lambda}$	$g_{K^* N \Lambda}$	$\kappa_{K^* N \Lambda}$	$g_{K^* N \Sigma}$	$\kappa_{K^* N \Sigma}$
6.56	7.45 GeV^{-1}	13.3	11.9	-13.4	-4.26	2.91	-2.46	-0.529

Exp.

SU(3) relation

Nijmegen potential (NSC97a)

Feynman Amplitudes



$$\mathcal{M} = \varepsilon_{\mu}^* \bar{u}_{\Lambda} \mathcal{M}^{\mu} u_N$$

$$\mathcal{M}_K^{\mu} = I_K \frac{i g_{\pi K K^*}}{t - M_K^2} \frac{g_{K N \Lambda}}{M_N + M_{\Lambda}} \gamma^{\nu} \gamma_5 k_1^{\mu} (k_2 - k_1)_{\nu},$$

$$\mathcal{M}_{K^*}^{\mu} = I_{K^*} \frac{g_{\pi K^* K^*} g_{K^* N \Lambda}}{t - M_{K^*}^2} \epsilon^{\mu\nu\alpha\beta} \left[\gamma_{\nu} - \frac{i \kappa_{K^* N \Lambda}}{M_N + M_{\Lambda}} \sigma_{\nu\lambda} (k_2 - k_1)^{\lambda} \right] k_{2\alpha} k_{1\beta},$$

$$\mathcal{M}_N^{\mu} = I_N \frac{i g_{K^* N \Lambda}}{s - M_N^2} \frac{g_{\pi N N}}{2 M_N} \left[\gamma^{\mu} - \frac{i \kappa_{K^* N \Lambda}}{M_N + M_{\Lambda}} \sigma^{\mu\nu} k_{2\nu} \right] (\not{k}_1 + \not{p}_1 + M_N) \gamma^{\alpha} \gamma_5 k_{1\alpha},$$

$$\mathcal{M}_{\Sigma}^{\mu} = I_{\Sigma} \frac{i g_{K^* N \Sigma}}{u - M_{\Sigma}^2} \frac{g_{\pi \Sigma \Lambda}}{M_{\Sigma} + M_{\Lambda}} \gamma^{\alpha} \gamma_5 (\not{p}_2 - \not{k}_1 + M_{\Sigma}) \left[\gamma^{\mu} - \frac{i \kappa_{K^* N \Sigma}}{M_N + M_{\Sigma}} \sigma^{\mu\nu} k_{2\nu} \right] k_{1\alpha}.$$

Feynman Amplitudes
& Cutoff Masses

$$\pi^- p \rightarrow K^{*0} \Lambda$$

$$\mathcal{M} = \mathcal{M}_K \cdot F_K + \mathcal{M}_{K^*} \cdot F_{K^*} \\ + \mathcal{M}_N \cdot F_N + \mathcal{M}_\Sigma \cdot F_\Sigma$$

$$\pi^- p \rightarrow D^{*-} \Lambda_c^+$$

$$\mathcal{M} = \mathcal{M}_D \cdot F_D + \mathcal{M}_{D^*} \cdot F_{D^*} \\ + \mathcal{M}_N \cdot F_N + \mathcal{M}_{\Sigma_c} \cdot F_{\Sigma_c}$$

$$F = \frac{\Lambda^4}{\Lambda^4 + (p^2 - M_{ex}^2)^2}$$

How to determine the cutoff masses, Λ ?

They are determined phenomenologically by fitting to the experimental data for the total and differential cross section.

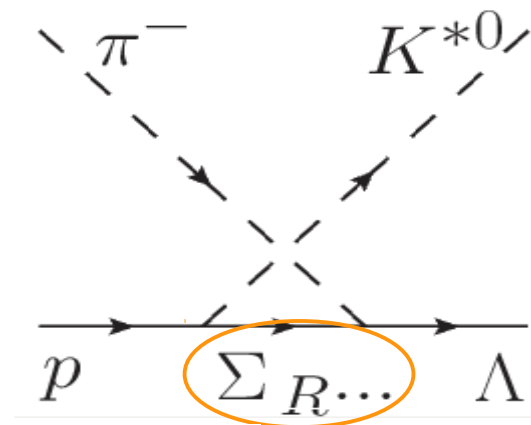
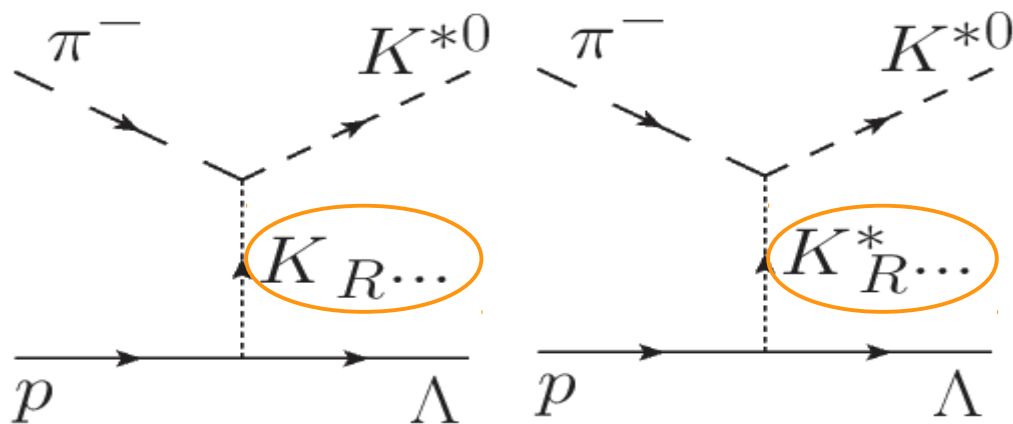


The same values are used.

$$\Lambda_{K,K^*} = 0.55 \text{ GeV} \\ \Lambda_{N,\Sigma} = 0.60 \text{ GeV}$$

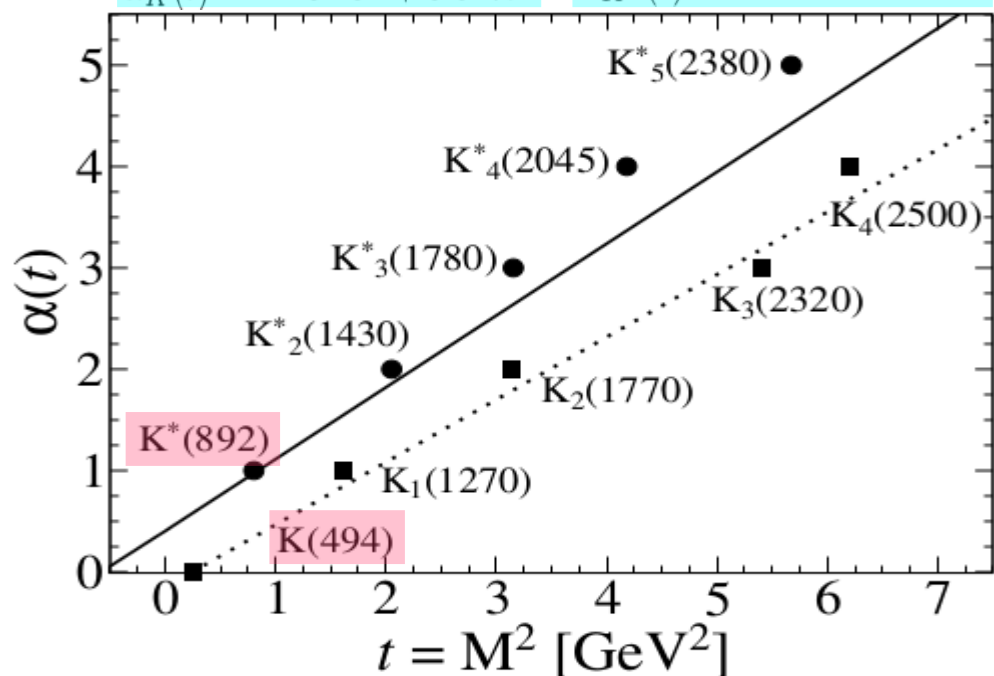
$$\left(\frac{d\sigma}{d\Omega} \right)_{\text{CM}} = \frac{1}{64\pi^2 s} \frac{\mathbf{p}_{out}}{\mathbf{k}_{in}} \frac{1}{2} \sum_{s,s'} |\mathcal{M}|^2$$

Regge Trajectories



$$\alpha_K(t) = -0.151 + 0.617t$$

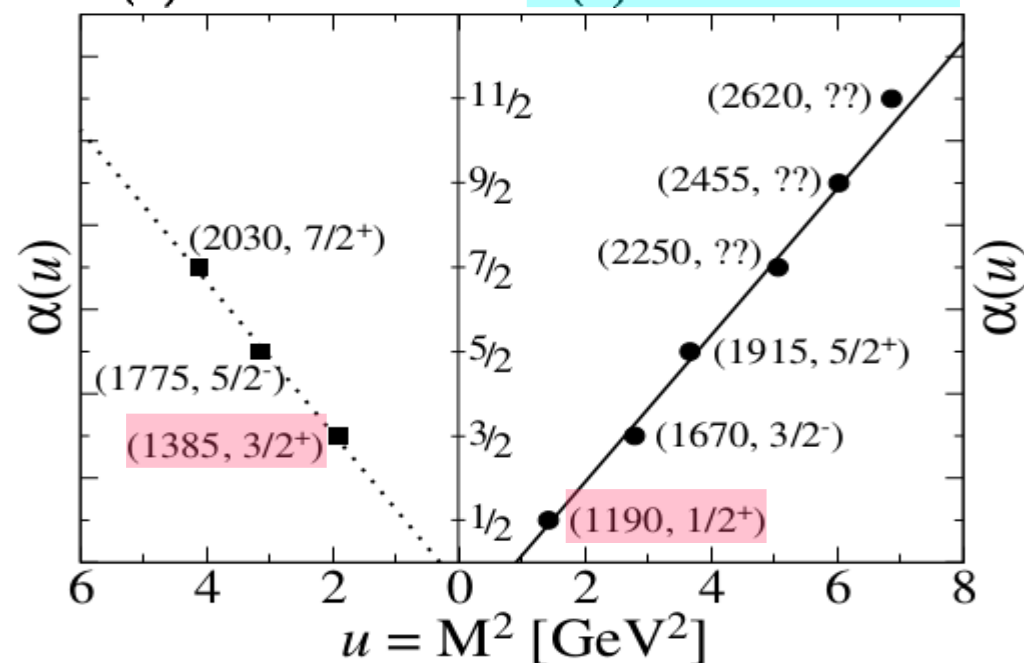
$$\alpha_{K^*}(t) = 0.414 + 0.707t$$



Brisudova et al, PRD 61.054013(2000)

$$\alpha(u) = -0.27 + 0.9u$$

$$\alpha(u) = -0.79 + 0.87u$$



J.K.Storow, PhysRept. 103.317(1984)

Regge Propagators (t channel)

$$P_K^F = \frac{1}{t - M_K^2} \Rightarrow P_K^R(s, t) = \left(\frac{1}{e^{-i\pi\alpha_K(t)}} \right) \left(\frac{s}{s_K} \right)^{\alpha_K(t)} \Gamma[-\alpha_K(t)] \alpha'_K,$$

$$P_{K^*}^F = \frac{1}{t - M_{K^*}^2} \Rightarrow P_{K^*}^R(s, t) = \left(\frac{1}{e^{-i\pi\alpha_{K^*}(t)}} \right) \left(\frac{s}{s_{K^*}} \right)^{\alpha_{K^*}(t)-1} \Gamma[1 - \alpha_{K^*}(t)] \alpha'_{K^*}$$

$$\frac{d\sigma}{dt}(s, t \rightarrow 0) \propto s^{2\alpha(t)-2} \quad \frac{d\sigma}{dt} = \frac{1}{64\pi(p_{\text{cm}})^2 s} \frac{1}{2} \sum_{s_i, s_f, \lambda_f} |\mathcal{M}|^2$$

\Rightarrow We introduce a normalization factor :

$$\mathcal{N}(s, t) = \frac{A^\infty(s)}{A(s, t)}, \quad A(s, t)^2 = \sum_{s_i, s_f, \lambda_f} |\mathcal{M}'(s, t)|^2$$

$$T_K(s, t) = \mathcal{M}_K(s, t) \mathcal{N}_K(s, t) P_K^R(s, t),$$

$$T_{K^*}(s, t) = \mathcal{M}_{K^*}(s, t) \mathcal{N}_{K^*}(s, t) P_{K^*}^R(s, t)$$

$$A_K^\infty = \frac{1}{\sqrt{2} M_{K^*}} (M_{K^*}^2 - M_\pi^2) (M_\Lambda - M_N)$$

$$\frac{\mathcal{M}_K \propto s^0}{\underline{\hspace{2cm}}}$$

$$A_{K^*}^\infty(s, t) = \sqrt{-2s^2 t} \longrightarrow \blacktriangleright A_{K^*}^\infty(s, t) = \sqrt{-2s^2 t} C(t)$$

$$\frac{\mathcal{M}_{K^*} \propto s^1}{\underline{\hspace{2cm}}}$$

Regge Propagators (u channel)

$$P_\Sigma^F = \frac{1}{u - M_\Sigma^2} \Rightarrow P_\Sigma^R(s, u) = \left(\frac{s}{s_\Sigma} \right)^{\alpha_\Sigma(u) - \frac{1}{2}} \Gamma \left[\frac{1}{2} - \alpha_\Sigma(u) \right] \alpha'_\Sigma$$

$$\frac{d\sigma}{du}(s, u \rightarrow 0) \propto s^{2\alpha(u) - 2} \quad \frac{d\sigma}{dt} = \frac{1}{64\pi(p_{\text{cm}})^2 s} \frac{1}{2} \sum_{s_i, s_f, \lambda_f} |\mathcal{M}|^2$$

=> We introduce a normalization factor :

$$\mathcal{N}(s, u) = \frac{A^\infty(s)}{A(s, u)}, \quad A(s, u)^2 = \sum_{s_i, s_f, \lambda_f} |\mathcal{M}'(s, u)|^2$$

$$T_\Sigma(s, u) = \mathcal{M}_\Sigma(s, u) \mathcal{N}_\Sigma(s, u) P_\Sigma^R(s, u)$$

$$A_\Sigma^\infty(s) = \sqrt{2s} \frac{M_\Lambda}{M_\Sigma + M_\Lambda} \left[M_\Sigma^2 (M_N^2 / M_{K^*}^2 + 2) + 6 \frac{\kappa_{K^* N \Sigma}}{M_\Sigma + M_N} M_N M_\Sigma^2 + \frac{\kappa_{K^* N \Sigma}^2}{(M_\Sigma + M_N)^2} M_\Sigma^2 (2M_N^2 + M_{K^*}^2) \right]^{\frac{1}{2}}$$

$\mathcal{M}_\Sigma \propto s^{\frac{1}{2}}$

$$\lim_{s \rightarrow \infty} \mathcal{N}_K(s, t) = \lim_{s \rightarrow \infty} \mathcal{N}_\Sigma(s, u) = 1$$

$$\lim_{s \rightarrow \infty} \mathcal{N}_{K^*}(s, t) = 0.6$$

[Titov, Kampfer PRC.78.025201(2008)]

$$\bar{p} p \rightarrow \bar{Y}_c Y_c \quad \text{and} \quad \bar{p} p \rightarrow M_c \bar{M}_c$$

Regge Propagators (charm)

$$T_{D^*}(s, t) = \mathcal{M}_{D^*}(s, t) \mathcal{N}_{D^*}(s, t) \left(\frac{s}{s_{D^*}} \right)^{\alpha_{D^*}(t)-1} \Gamma[1 - \alpha_{D^*}(t)] \alpha'_{D^*}$$

$$T_{\Sigma_c}(s, u) = \mathcal{M}_{\Sigma_c}(s, u) \mathcal{N}_{\Sigma_c}(s, u) \left(\frac{s}{s_{\Sigma_c}} \right)^{\alpha_{\Sigma_c}(u)-\frac{1}{2}} \Gamma\left[\frac{1}{2} - \alpha_{\Sigma_c}(u)\right] \alpha'_{\Sigma_c}$$

Regge Parameters

(a) Regge trajectories : $\alpha(t) = \alpha(0) + \alpha' t$ $\alpha(u) = \alpha(0) + \alpha' u$

(b) Energy scale parameters : $s_0^{\pi N \rightarrow K^* \Lambda}$ $s_0^{\pi N \rightarrow D^* \Lambda_c}$

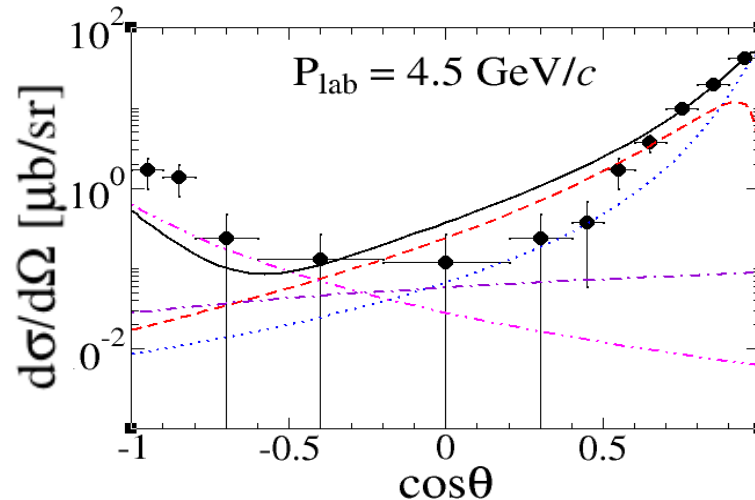
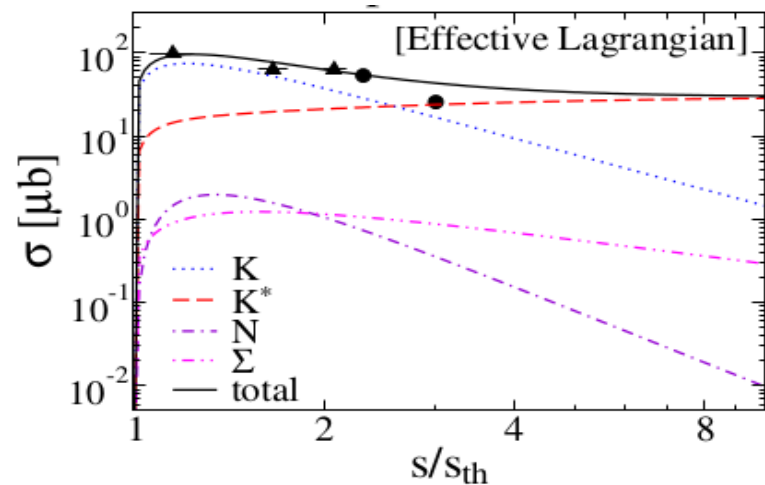
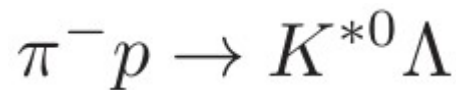
=> determined by using **Quark-Gluon-String Model(QGSM)**.

[Kaidalov, ZphysC.12.63(1982), Brisudova et al, PRD61.054013(2000)]

(c) Residual factor C(t) in K^* reggeon :

$$\Rightarrow C(t) = \frac{0.6}{1 - t/\Lambda^2} \quad \Lambda = \underline{1} \sim 1.5 \text{ [GeV]}$$

I. 3. Results : Total & Differential Cross Sections

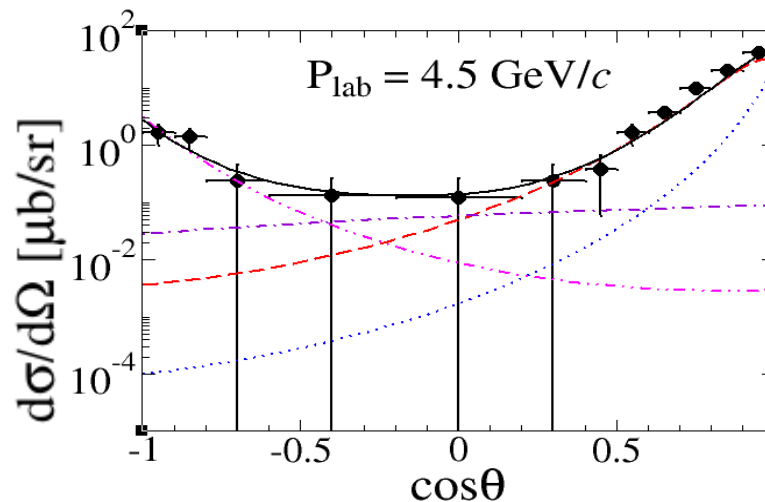
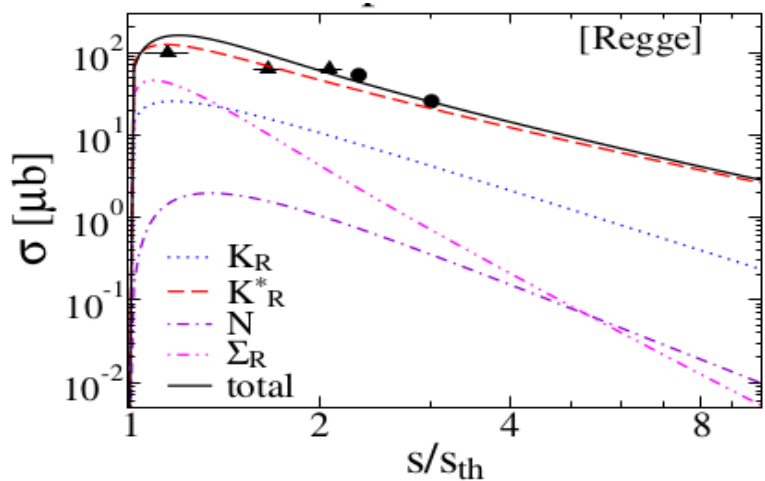


Exp. Data :
 Dahl et al,
 PR163.1377(1967)
 Crennell et al,
 PRD6.1220(1972)

$$\sigma \sim s^{J-1}$$

K exchange contributes mainly to the low-energy region, whereas K^* exchange comes into play when s/s_{th} gets large.

[Effective Lagrangians]



[Regge]

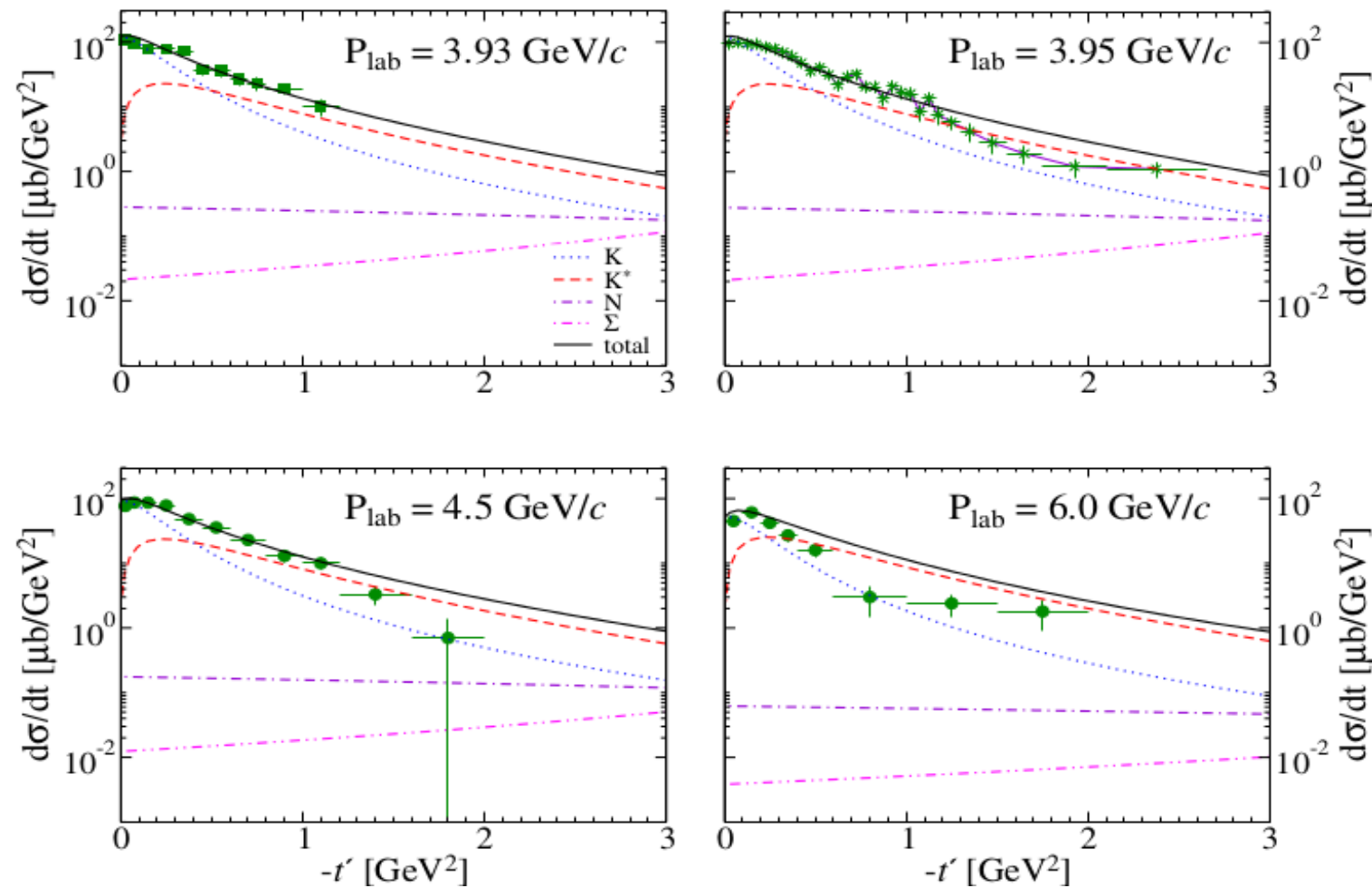
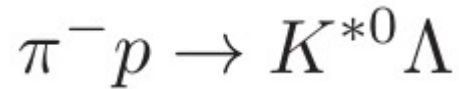
$$T \sim s^{\alpha(0)}$$

$$T_{K^*} \sim s^{0.414}$$

$$T_{\Sigma} \sim s^{-0.79}$$

K^* reggeon is dominant in the whole energy region. As s increases, the intercepts $\alpha(0)$ play decisive roles in explaining the experimental data.

I. 3. Results : Differential Cross Sections [Effective Lagrangians]



Exp. Data :

Yaffe et al,
NPB75.365(1974)

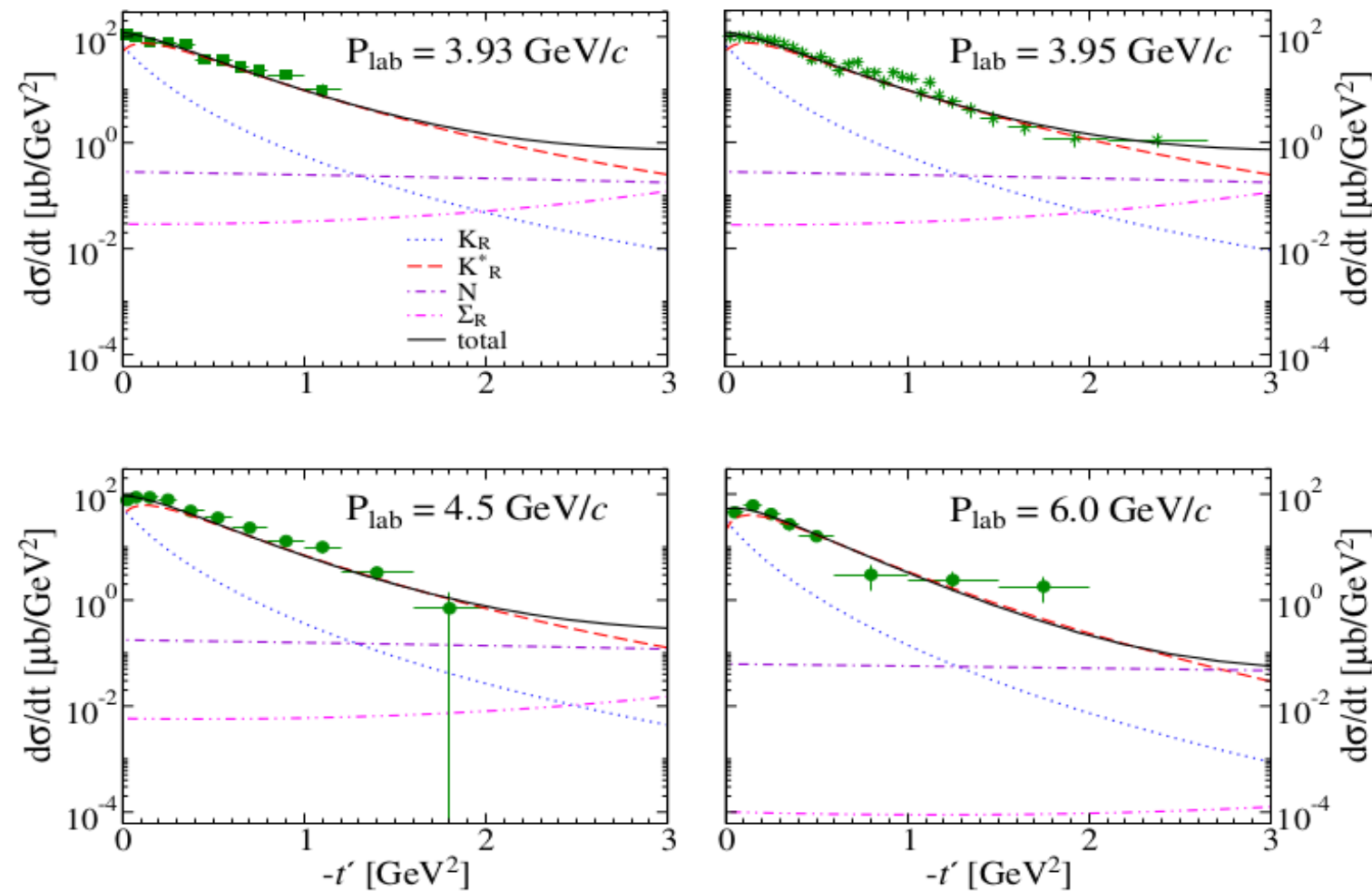
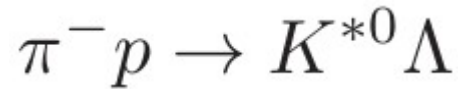
Aguilar-Benitez et al,
ZPhysikC6.195(1980)

Crennell et al,
PRD6.1220(1972)

K exchange governs $d\sigma/dt$ near $-t' \approx 0$, whereas K^* exchange becomes the main contribution.

The results fit the experimental data between $0 < -t' < 1.2$ [GeV^2], they start to deviate from the data as $-t'$ increases.

I. 3. Results : Differential Cross Sections [Regge]



Exp. Data :

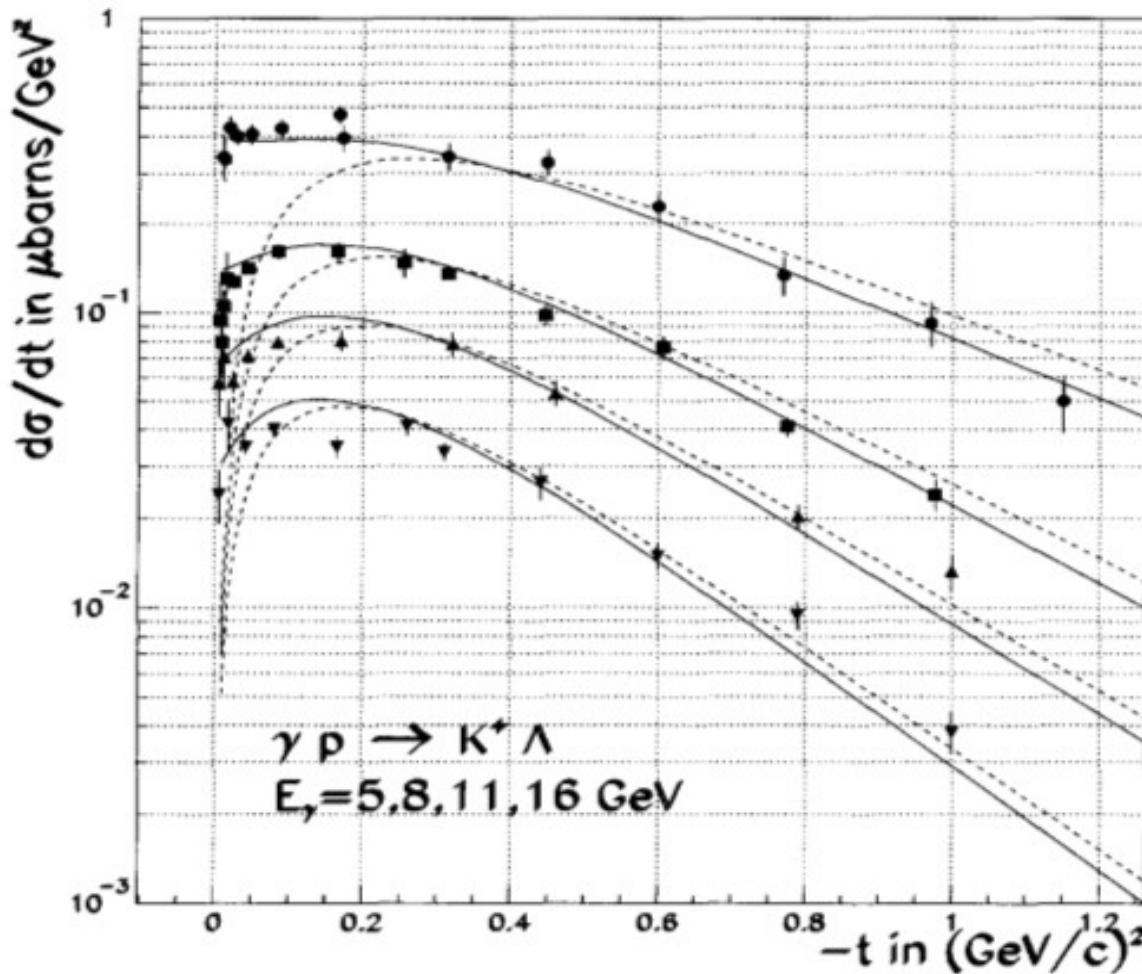
Yaffe et al,
NPB75.365(1974)

Aguilar-Benitez et al,
ZPhysikC6.195(1980)

Crennell et al,
PRD6.1220(1972)

The results fall off faster than those from the effective Lagrangian method, as t' increases. The Regge approach explains the experimental data better at higher values of p_{lab} .

I. 3. Results : Examples

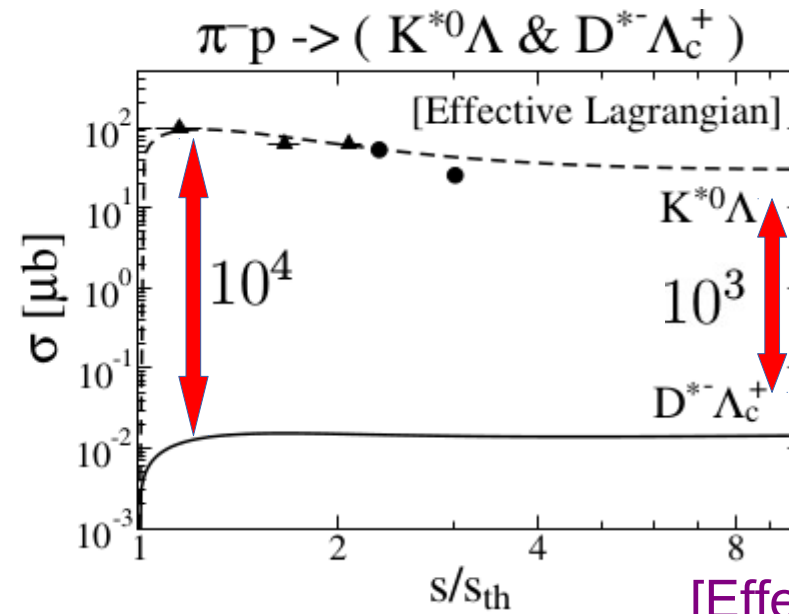
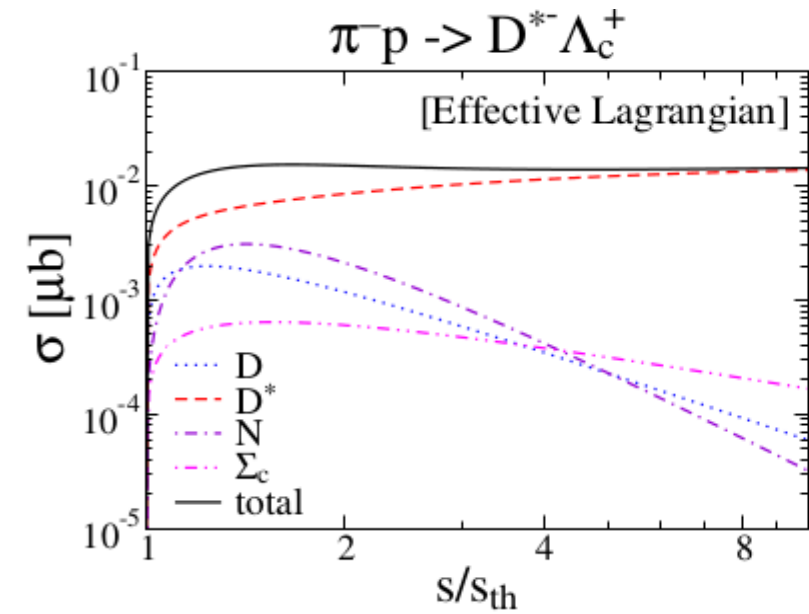


Guidal et al,
NuclPhysA.627.645(1997)

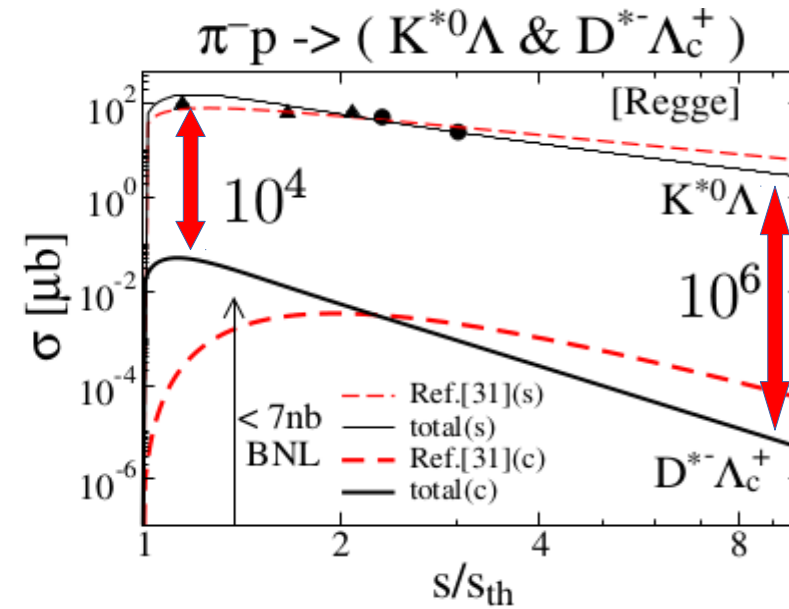
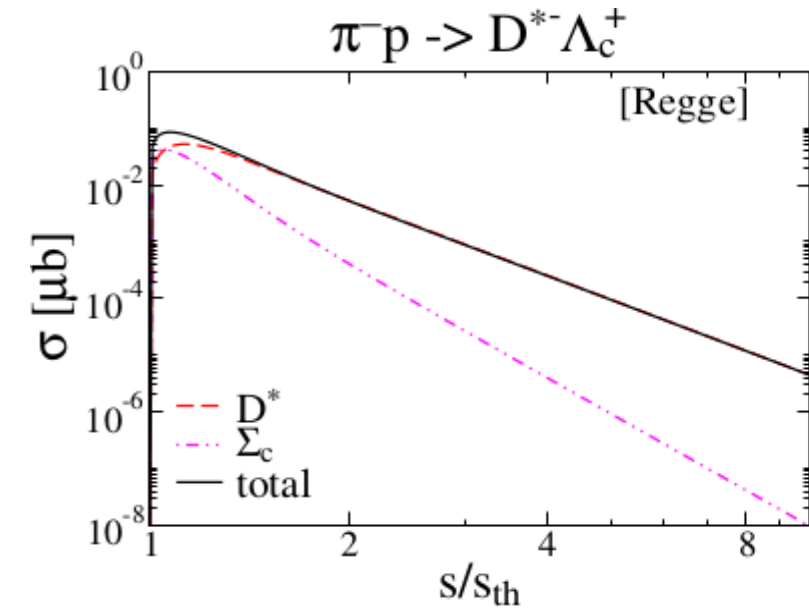
dashed curves : K^* -reggeon exchange contribution.

full curves : Gauge invariant $K+K^*$ reggeon exchange model.

I. 3. Results : Total Cross Sections



[Effective Lagrangians]

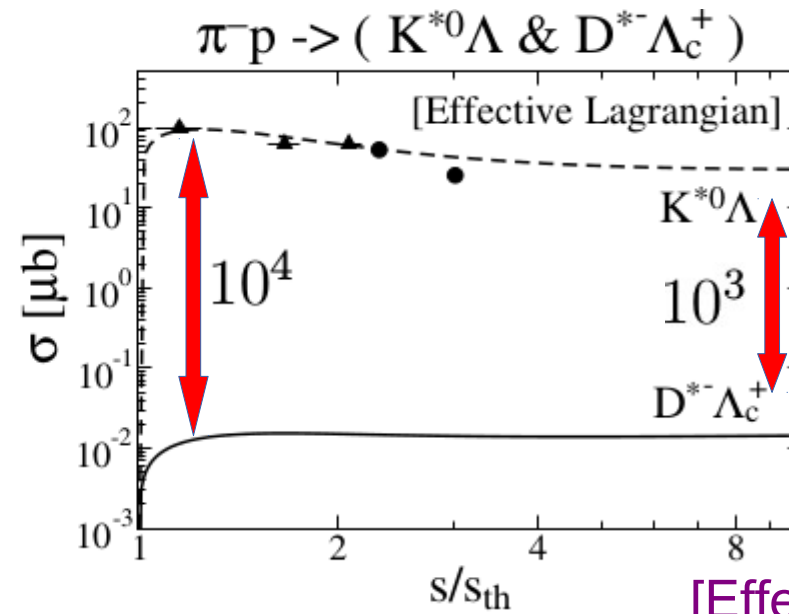
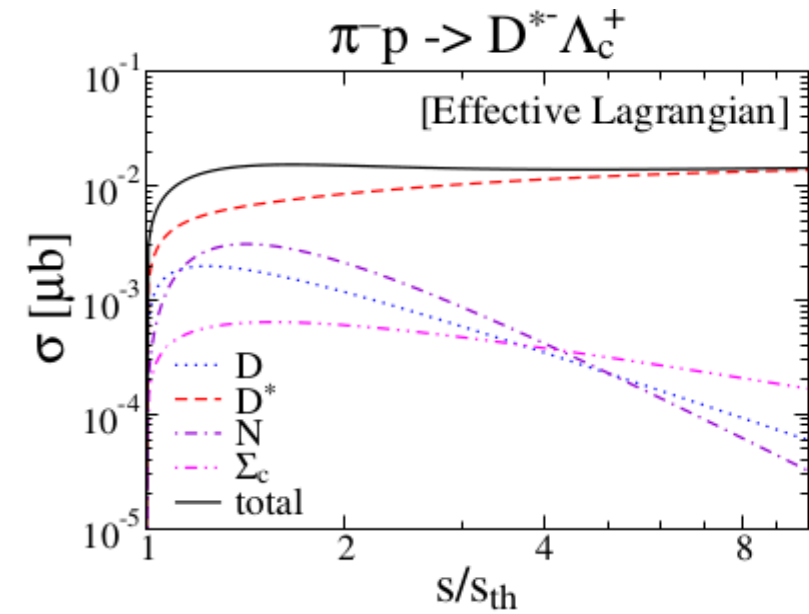


[Regge]

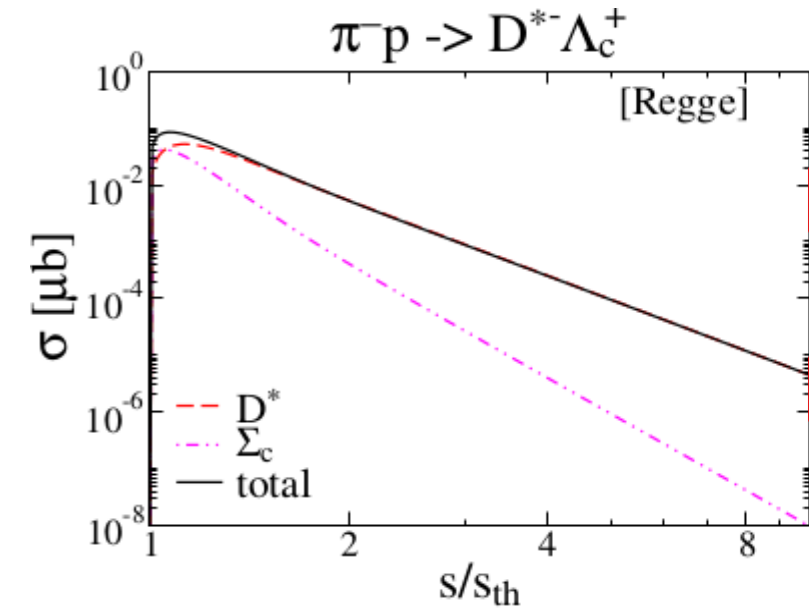
Grishina et al,
EurPhysJA.25.141(2005)

$$\sigma = \int C \frac{g_{\pi K^* K}^2 g_{K^* N \Lambda}^2}{64\pi (p_{\text{cm}})^2 s} \exp(2R^2 t) \left(\frac{s}{s_{\text{th}}} \right)^{2\alpha_{K^*}(t)} dt$$

I. 3. Results : Total Cross Sections

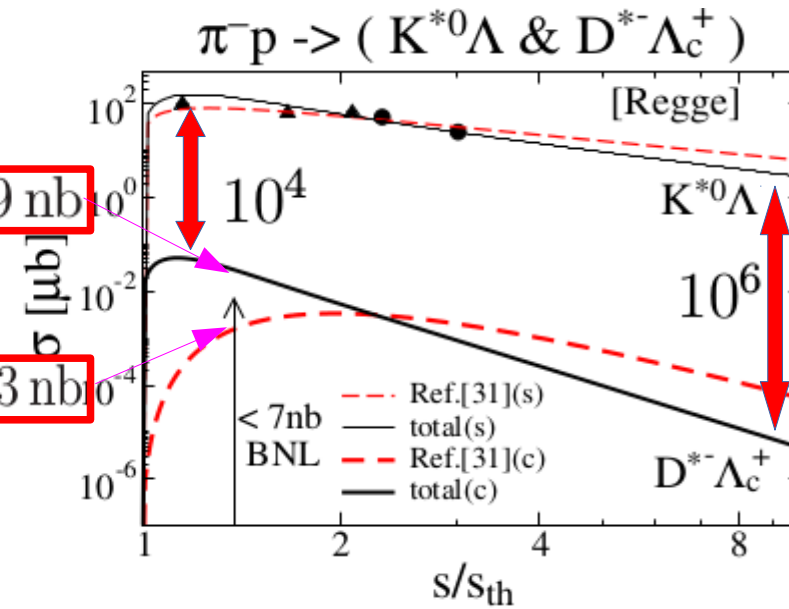


[Effective Lagrangians]



29 nb

2.3 nb



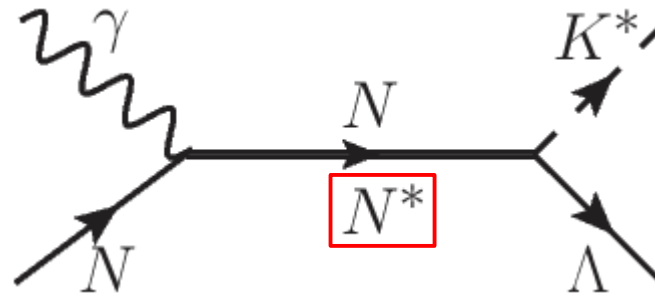
[Regge]

Grishina et al,
EurPhysJA.25.141(2005)

$$\sigma = \int C \frac{g_{\pi K^* K}^2 g_{K^* N \Lambda}^2}{64\pi (p_{\text{cm}})^2 s} \exp(2R^2 t) \left(\frac{s}{s_{\text{th}}} \right)^{2\alpha_{K^*}(t)} dt$$

$$\mathbb{I} . \quad \gamma N \rightarrow K^* \Lambda$$

$$\gamma N \rightarrow K^* \Lambda$$



- ◇ Present work contains the N^* resonances of [the PDG 2010 edition](#).
[PRD.84.114023, S.H.Kim, et al. (2011)]

- ◇ In [the PDG 2012 edition](#), Anisovich et al. performed a multichannel partial wave analysis taking both the πN and various photoproduction data, in particular, reactions like,

$$\gamma p \rightarrow p\pi^0, n\pi^+, p\eta, p\pi^0\pi^0, p\pi^+\pi^-, p\pi^0\eta, \Lambda K^+, \Sigma^0 K^+, \text{ and } \Sigma^+ K_s^0$$

[EPJA.48.15, A.V.Anisovich, et al. (2012)
 PLB.711.162, A.V.Anisovich, et al. (2012)
 PLB.711.167, A.V.Anisovich, et al. (2012)]

- ◇ A few new N^* resonances were included and some were rearranged in the N^* spectrum.

II. 1. Motivation

$$\gamma N \rightarrow K^* \Lambda$$

PDG (2010)

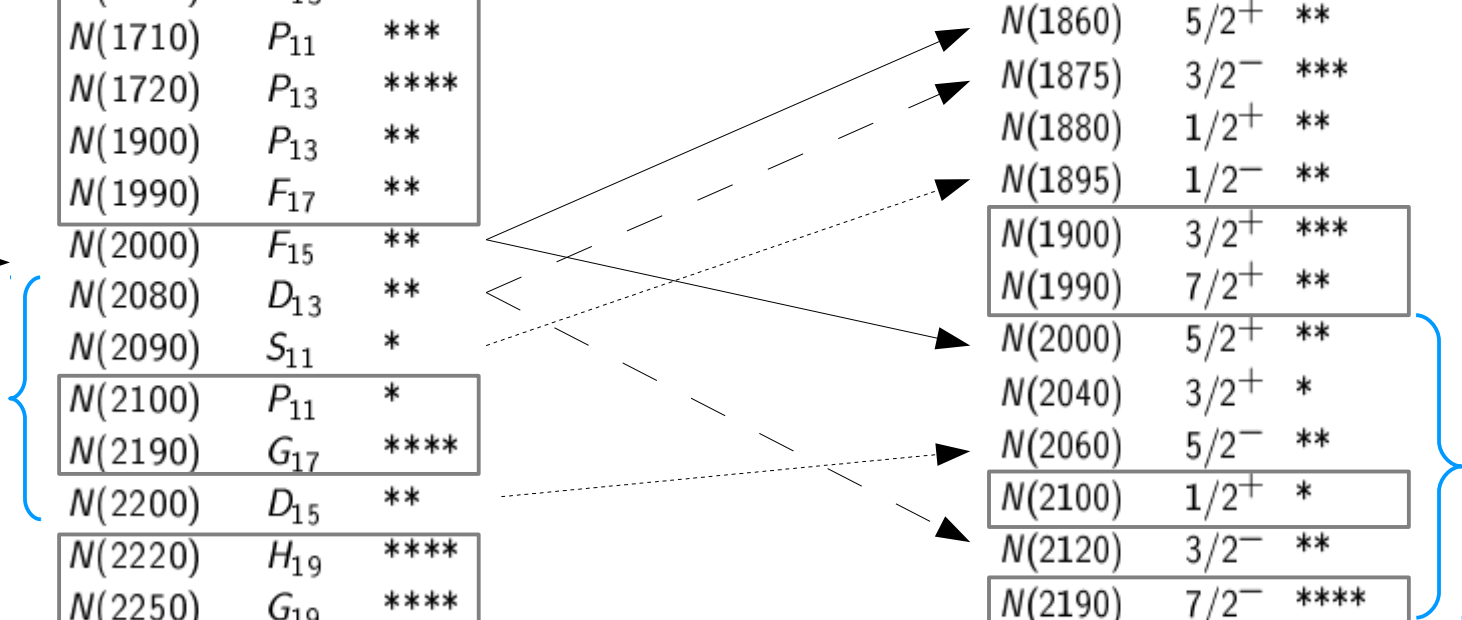
$N(1440)$	P_{11}	****
$N(1520)$	D_{13}	****
$N(1535)$	S_{11}	****
$N(1650)$	S_{11}	****
$N(1675)$	D_{15}	****
$N(1680)$	F_{15}	****
$N(1700)$	D_{13}	***
$N(1710)$	P_{11}	***
$N(1720)$	P_{13}	****
$N(1900)$	P_{13}	**
$N(1990)$	F_{17}	**
$N(2000)$	F_{15}	**
$N(2080)$	D_{13}	**
$N(2090)$	S_{11}	*
$N(2100)$	P_{11}	*
$N(2190)$	G_{17}	****
$N(2200)$	D_{15}	**
$N(2220)$	H_{19}	****
$N(2250)$	G_{19}	****
$N(2600)$	$l_{1,11}$	***
$N(2700)$	$K_{1,13}$	**

PDG (2012)

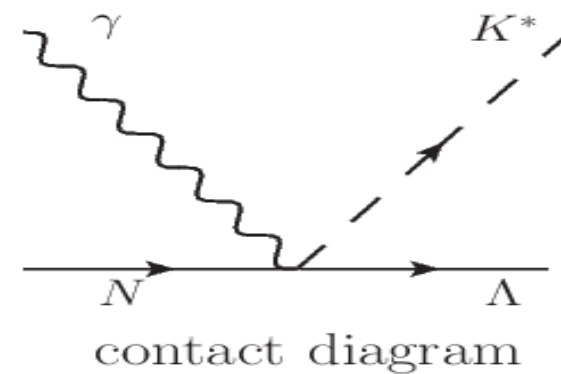
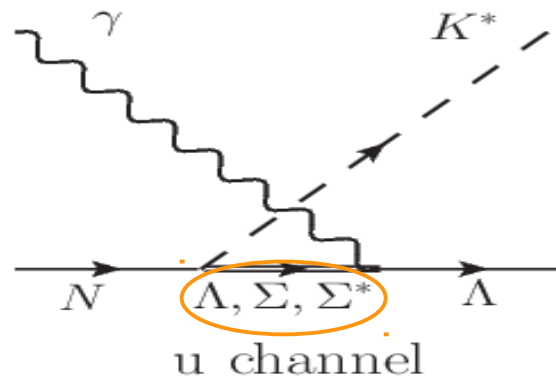
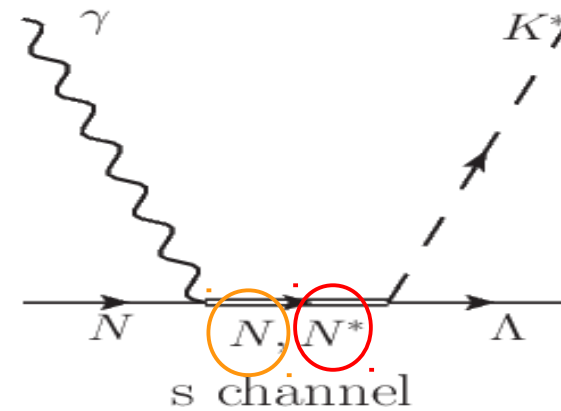
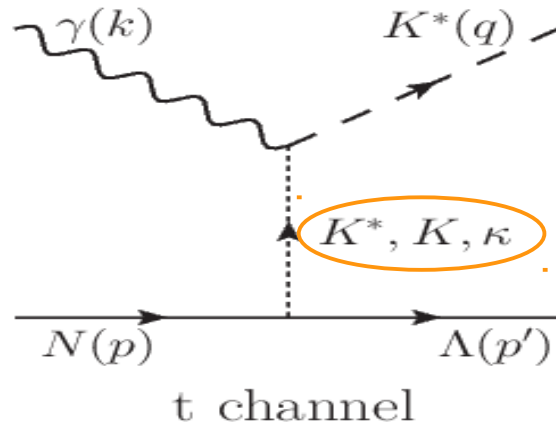
$N(1440)$	$1/2^+$	****
$N(1520)$	$3/2^-$	****
$N(1535)$	$1/2^-$	****
$N(1650)$	$1/2^-$	****
$N(1675)$	$5/2^-$	****
$N(1680)$	$5/2^+$	****
$N(1685)$		*
$N(1700)$	$3/2^-$	***
$N(1710)$	$1/2^+$	***
$N(1720)$	$3/2^+$	****
$N(1860)$	$5/2^+$	**
$N(1875)$	$3/2^-$	***
$N(1880)$	$1/2^+$	**
$N(1895)$	$1/2^-$	**
$N(1900)$	$3/2^+$	***
$N(1990)$	$7/2^+$	**
$N(2000)$	$5/2^+$	**
$N(2040)$	$3/2^+$	*
$N(2060)$	$5/2^-$	**
$N(2100)$	$1/2^+$	*
$N(2120)$	$3/2^-$	**
$N(2190)$	$7/2^-$	****
$N(2220)$	$9/2^+$	****
$N(2250)$	$9/2^-$	****
$N(2600)$	$11/2^-$	***
$N(2700)$	$13/2^+$	**

$K^* \Lambda$ threshold

$K^* \Lambda$ threshold

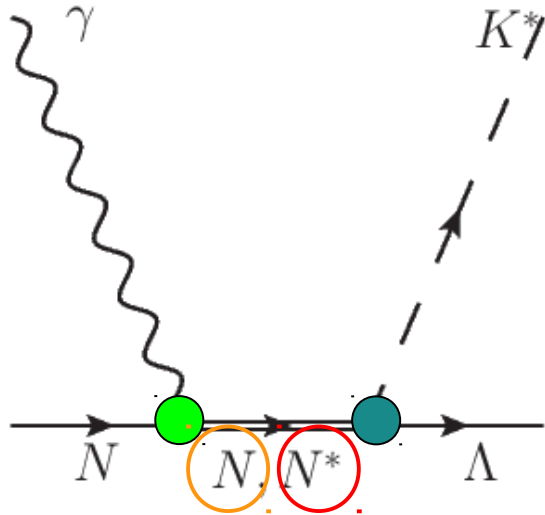


Tree Level Diagrams



- ◆ Each of the interaction vertices is defined by **the effective Lagrangians**.
- ◆ The contact term is necessary to satisfy the WT identity.

s-channel



$$\Gamma_{\mu}^{(\pm)} = \begin{pmatrix} \gamma_{\mu} \gamma_5 \\ \gamma_{\mu} \end{pmatrix}, \quad \Gamma^{(\pm)} = \begin{pmatrix} \gamma_5 \\ 1 \end{pmatrix}$$

N exchange

$$\mathcal{L}_{\gamma NN} = -e\bar{N} \left[\gamma_{\mu} A^{\mu} \frac{1 + \tau_3}{2} - \frac{1}{2M_N} (\kappa_s^N + \kappa_v^N \tau_3) \sigma_{\mu\nu} \partial^{\nu} A^{\mu} \right] N$$

N* exchange

$$\mathcal{L}_{\gamma NN^*} \left(\frac{3^{\pm}}{2} \right) = -\frac{ieh_1}{2M_N} \bar{N} \Gamma_{\nu}^{(\pm)} F^{\mu\nu} N_{\mu}^* - \frac{eh_2}{(2M_N)^2} \partial_{\nu} \bar{N} \Gamma^{(\pm)} F^{\mu\nu} N_{\mu}^* + \text{H.c.},$$

$$\mathcal{L}_{\gamma NN^*} \left(\frac{5^{\pm}}{2} \right) = \frac{eh_1}{(2M_N)^2} \bar{N} \Gamma_{\nu}^{(\mp)} \partial^{\alpha} F^{\mu\nu} N_{\mu\alpha}^* - \frac{ieh_2}{(2M_N)^3} \partial_{\nu} \bar{N} \Gamma^{(\mp)} \partial^{\alpha} F^{\mu\nu} N_{\mu\alpha}^* + \text{H.c.}$$

$$\mathcal{L}_{K^* N^* \Lambda} \left(\frac{3^{\pm}}{2} \right) = -\frac{g_{1D_{13}}}{2M_N} \bar{\Lambda} \Gamma_{\nu}^{(\pm)} K^{*\mu\nu} N_{\mu}^* - \frac{g_{2D_{13}}}{(2M_N)^2} \partial_{\nu} \bar{\Lambda} \Gamma^{(\pm)} K^{*\mu\nu} N_{\mu}^* + \frac{g_{3D_{13}}}{(2M_N)^2} \bar{\Lambda} \Gamma^{(\pm)} \partial_{\nu} K^{*\mu\nu} N_{\mu}^* + \text{H.c.},$$

$$\mathcal{L}_{K^* N^* \Lambda} \left(\frac{5^{\pm}}{2} \right) = \frac{g_{1D_{15}}}{(2M_N)^2} \bar{\Lambda} \Gamma_{\nu}^{(\mp)} \partial^{\alpha} K^{*\mu\nu} N_{\mu\alpha}^* - \frac{g_{2D_{15}}}{(2M_N)^3} \partial_{\nu} \bar{\Lambda} \Gamma^{(\mp)} \partial^{\alpha} K^{*\mu\nu} N_{\mu\alpha}^* + \frac{ig_{3D_{15}}}{(2M_N)^3} \bar{\Lambda} \Gamma^{(\mp)} \partial^{\alpha} \partial_{\nu} K^{*\mu\nu} N_{\mu\alpha}^* + \text{H.c.}$$

- ◆ The transition magnetic moments h_{N^*} and the helicity amplitudes A_{N^*} are related linearly.

[A.V. Anisovich et al, EPJA. 48. 15 (2012)

A.V. Anisovich et al, EPJA. 49. 67 (2013)

S. Capstick, PRD. 46. 2864 (1992)]

proton(neutron) target

PDG	M_{BW}	Γ_{BW}	A_1	A_3	h_1	h_2
$N(2000)5/2^+$	2090	460	+32(-18)	+48(-35)	+0.114(-0.395)	+1.22(-0.500)
$N(2060)5/2^-$	2060	375	+67(+25)	+55(-37)	-2.45(+0.027)	-3.81(-2.85)
$N(2120)3/2^-$	2150	330	+130(+110)	+150(+40)	-0.827(-1.66)	+2.14(+2.31)
$N(2190)7/2^-$	2180	335	-34(+10)	+28(-14)	+7.87(-2.94)	-7.36(+2.49)

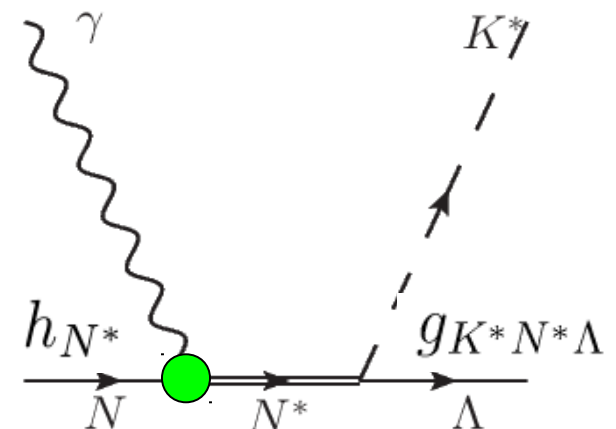
$$\Gamma(R \rightarrow N\gamma) = \frac{k_\gamma^2}{\pi} \frac{2M_N}{(2j+1)M_R} [|A_{1/2}|^2 + |A_{3/2}|^2]$$

$$\frac{1}{2}^\pm \rightarrow A_{1/2}(\frac{1}{2}^\pm) = \mp \frac{eh_1}{2M_N} \sqrt{\frac{k_\gamma M_R}{M_N}}$$

$$\frac{3}{2}^\pm \rightarrow A_{1/2}(\frac{3}{2}^\pm) = \mp \frac{e\sqrt{6}}{12} \sqrt{\frac{k_\gamma}{M_N M_R}} \left[h_1 \mp \frac{h_2}{4M_N^2} M_R (M_R \mp M_N) \right]$$

$$A_{3/2}(\frac{3}{2}^\pm) = \mp \frac{e\sqrt{2}}{4M_N} \sqrt{\frac{k_\gamma M_R}{M_N}} \left[h_1 \mp \frac{h_2}{4M_N} (M_R \mp M_N) \right]$$

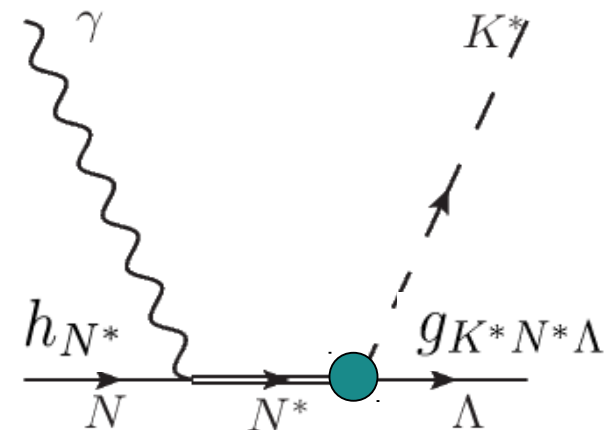
units of $10^{-3} \text{GeV}^{-\frac{1}{2}}$



- ◆ We assume that N(2000), N(2060), N(2120), and N(2190) may correspond respectively to F₁₅(2000), D₁₅(2000), D₁₃(2080), and G₁₇(2190) in the PDG 2010 edition.
- ◆ The coupling strength of $g_{K^*N^*\Lambda}$ is obtained using the SU(6) quark model.
[S.Capstick and W.Roberts, PRD58, 074011 (1998)]

$$\Gamma(N^* \rightarrow K^* \Lambda) = \sum_{l,s} |G(l, s)|^2$$

PDG	M _{BW}	Γ _{BW}	G(l, s)	g ₁	g ₁ (final)
N(2000)5/2 ⁺	2090	460	+0.3	+1.37	+1.37
N(2060)5/2 ⁻	2060	375	+0.2	+5.42	+5.42
N(2120)3/2 ⁻	2150	330	+3.8	+1.29	+0.30
N(2190)7/2 ⁻	2180	335	+2.5	-44.3	-44.3



Amplitude with Form factors

$$\underline{\gamma p \rightarrow K^{+*} \Lambda}$$

$$M_p = (M_{K^*} + M_p + M_C)F_C^2 + M_K F_K^2 + M_\kappa F_\kappa^2 + M_\Lambda F_\Lambda^2 + M_\Sigma F_\Sigma^2 + M_{\Sigma^*} F_{\Sigma^*}^2 + M_{p^*} F_{p^*}^2$$

$$\underline{\gamma n \rightarrow K^{0*} \Lambda}$$

$$M_n = M_K F_K^2 + M_\kappa F_\kappa^2 + M_n F_n^2 + M_\Lambda F_\Lambda^2 + M_\Sigma F_\Sigma^2 + M_{\Sigma^*} F_{\Sigma^*}^2 + M_{n^*} F_{n^*}^2$$

Form factor

t-channel

s-, u-channel

common form factor

$$F_M(p^2) = \frac{\Lambda^2 - M_{ex}^2}{\Lambda^2 - p^2}$$

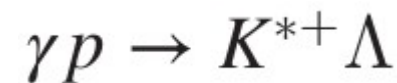
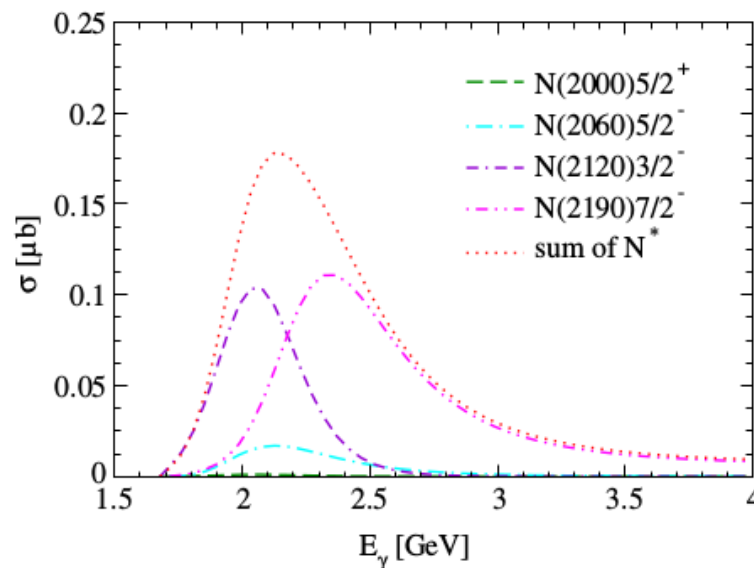
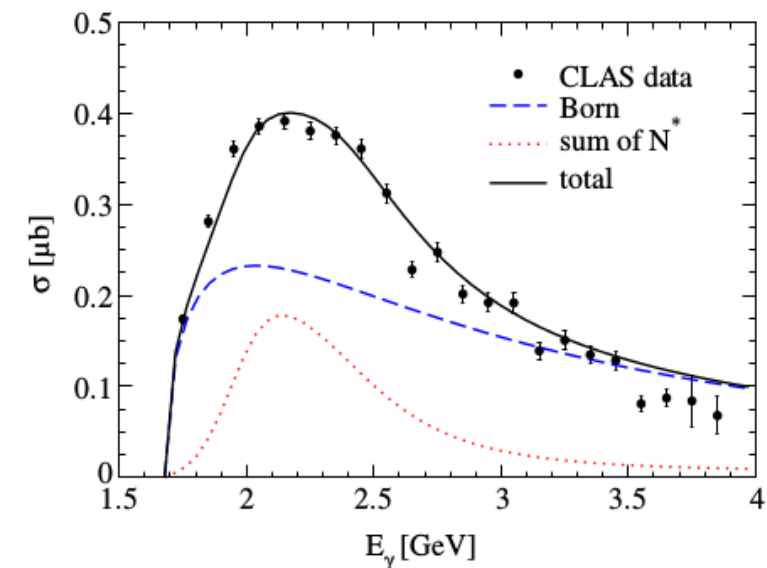
$$F_B(p^2) = \frac{\Lambda^4}{\Lambda^4 + (p^2 - M_{ex}^2)^2}$$

$$F_C = F_p F_{K^*} - F_p - F_{K^*}$$

- ◆ The cutoff values, Λ are determined phenomenologically :

$$\Lambda_{K^*, N, \Lambda, \Sigma, \Sigma^*} = 0.9 \text{ GeV}, \Lambda_{K, \kappa} = 1.1 \text{ GeV}, \text{ and } \Lambda_R = 1.0 \text{ GeV}.$$

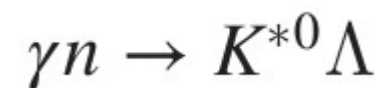
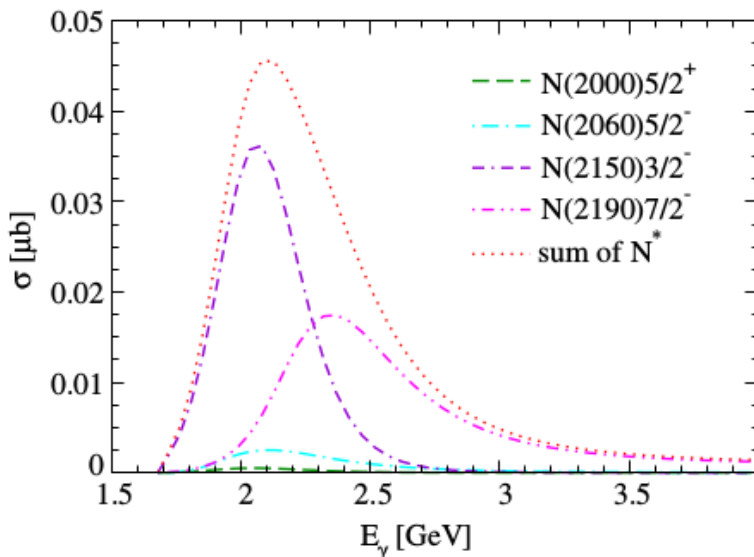
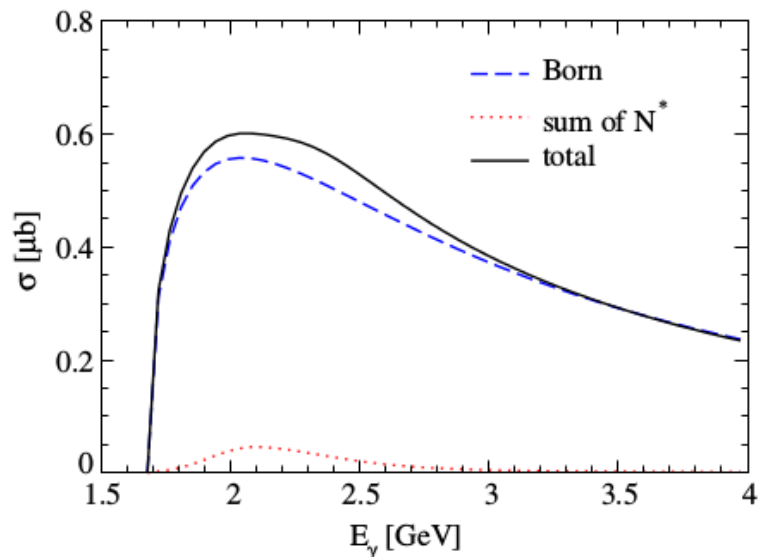
II. 3. Results : Total Cross Sections



Exp. Data :
W.Tang, et al,
PRC87.065204(2013)

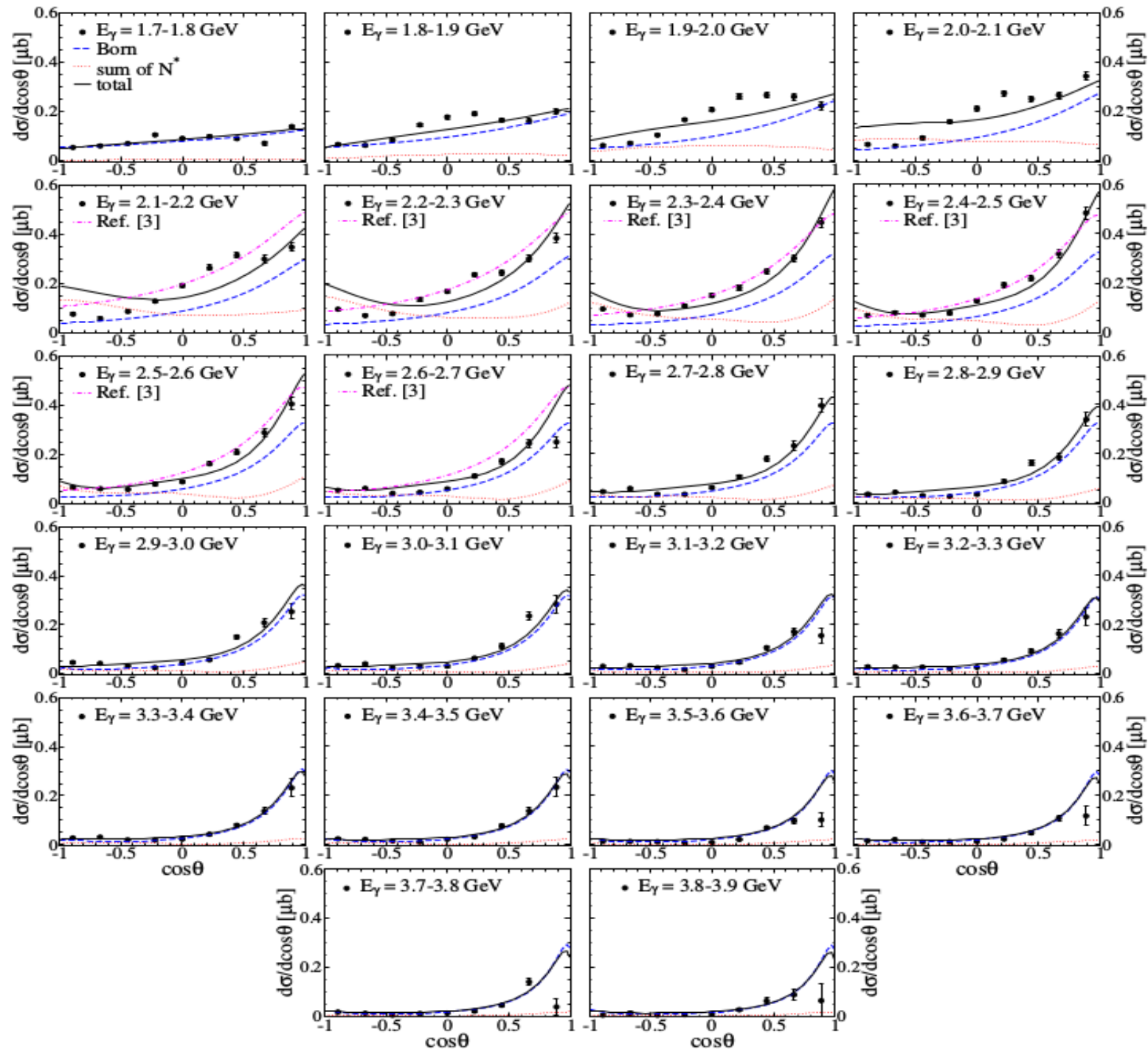
S.H.Kim, et al,
PRD90.014021(2014)

N(2190)7/2⁻ turns out to be equally as important as N(2120)3/2⁻.
It governs the dependence of the TCS on the E_γ in higher E_γ regions.



The main contribution arises from the K exchange.
The effects of the N* resonances are almost marginal.

II. 3. Results : Differential Cross Sections $\gamma p \rightarrow K^{*+} \Lambda$



II. 3. Results : Polarization Observables

The polarization observables, which provide crucial information on the helicity amplitudes and spin structure of a process :

B(photon beam),
 T(target nucleon),
 R(recoil Λ),
 V(produced K^* meson)

1. Single polarization observables :

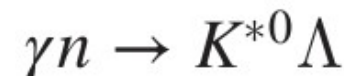
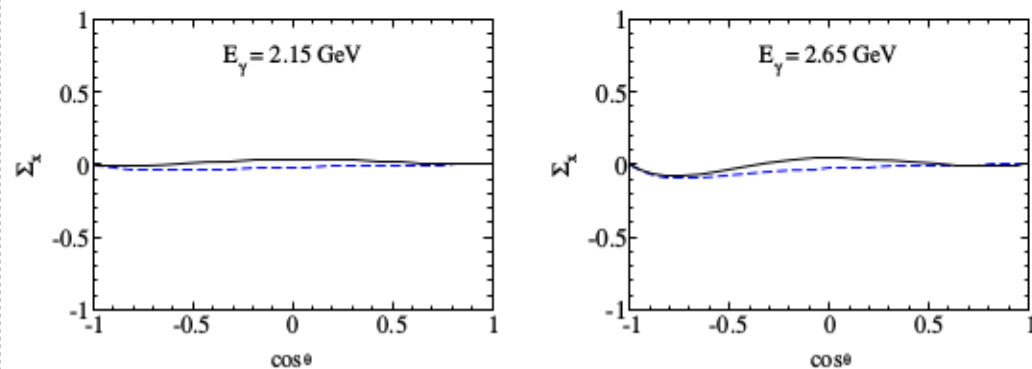
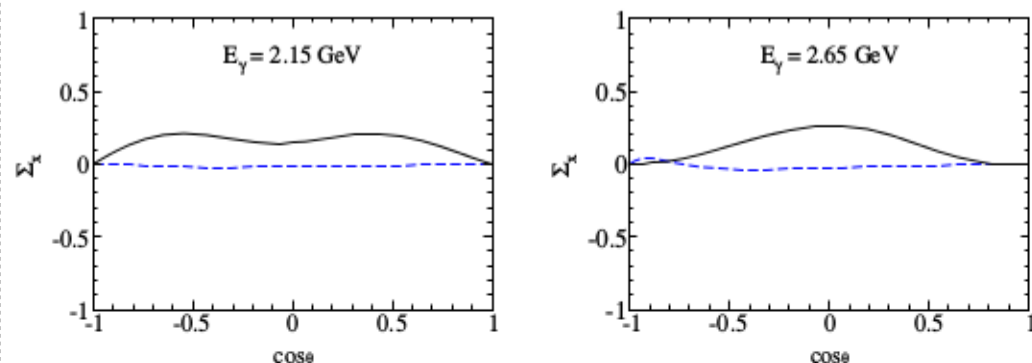
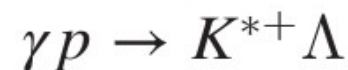
$$d\sigma(B, T; R, V) = \frac{d\sigma}{d\Omega}(B, T; R, V)$$

$$\Sigma_x = \frac{d\sigma(\perp, U; U, U) - d\sigma(\parallel, U; U, U)}{d\sigma(\perp, U; U, U) + d\sigma(\parallel, U; U, U)},$$

$$T_y = \frac{d\sigma(U, y; U, U) - d\sigma(U, -y; U, U)}{d\sigma(U, y; U, U) + d\sigma(U, -y; U, U)},$$

$$P_y = \frac{d\sigma(U, U; y, U) - d\sigma(U, U; -y, U)}{d\sigma(U, U; y, U) + d\sigma(U, U; -y, U)},$$

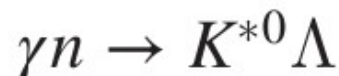
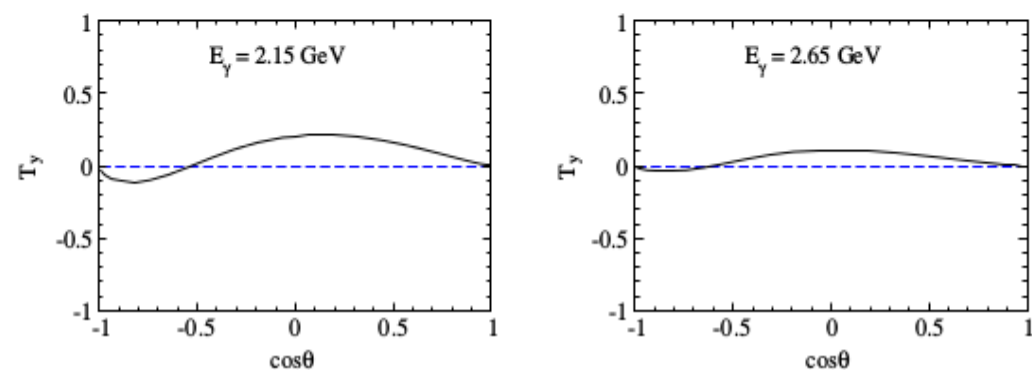
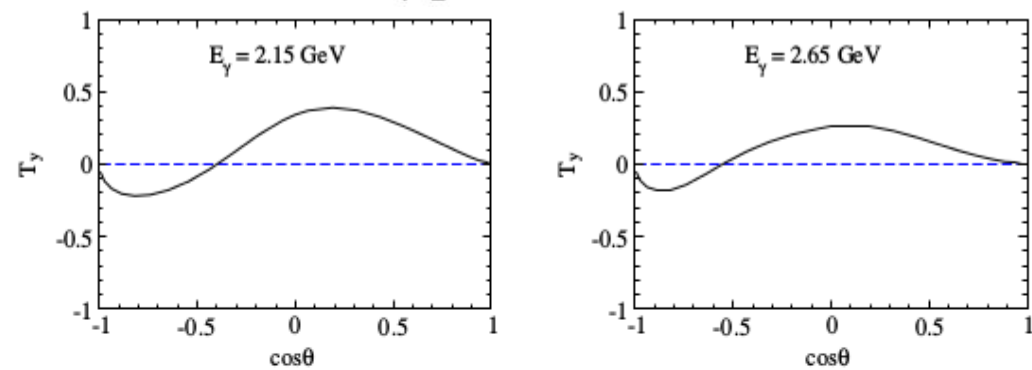
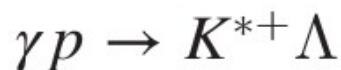
1.1. Photon-Beam Asymmetry (B)



$$\Sigma_x = \frac{d\sigma(\perp, U; U, U) - d\sigma(\parallel, U; U, U)}{d\sigma(\perp, U; U, U) + d\sigma(\parallel, U; U, U)}$$

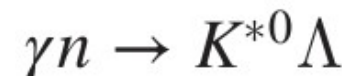
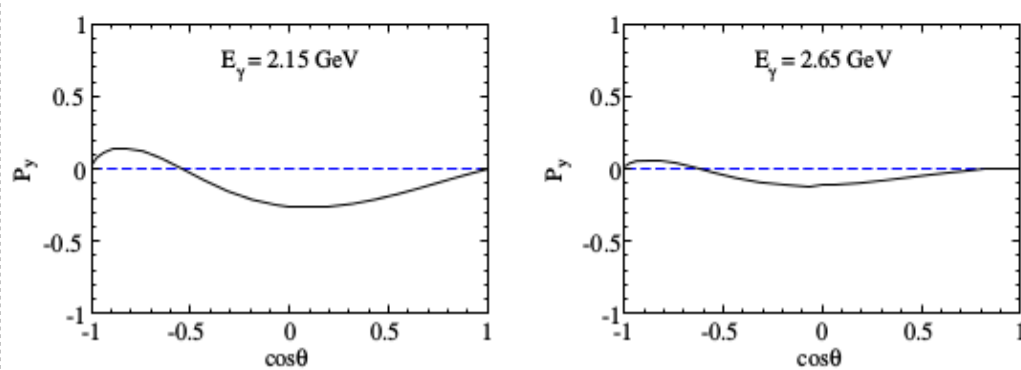
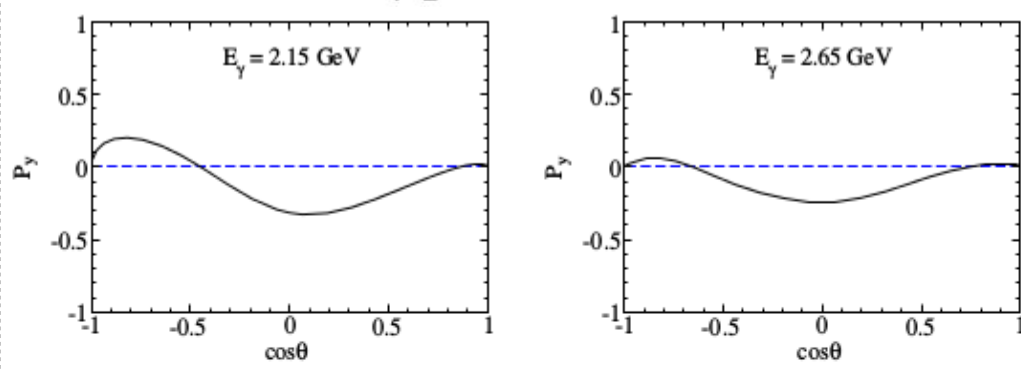
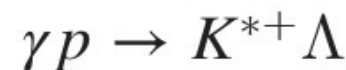
II. 3. Results : Polarization Observables

1.2. Target Asymmetry (T_y)



$$T_y = \frac{d\sigma(U, y; U, U) - d\sigma(U, -y; U, U)}{d\sigma(U, y; U, U) + d\sigma(U, -y; U, U)}$$

1.3. Recoil Asymmetry (P_y)



$$P_y = \frac{d\sigma(U, U; y, U) - d\sigma(U, U; -y, U)}{d\sigma(U, U; y, U) + d\sigma(U, U; -y, U)}$$

II. 3. Results : Polarization Observables

2. Double polarization observables :

$$d\sigma(B, T; R, V) = \frac{d\sigma}{d\Omega}(B, T; R, V)$$

$$C_{zz}^{\text{TR}} = \frac{d\sigma(U, z; z, U) - d\sigma(U, z; -z, U)}{d\sigma(U, z; z, U) + d\sigma(U, z; -z, U)},$$

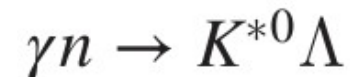
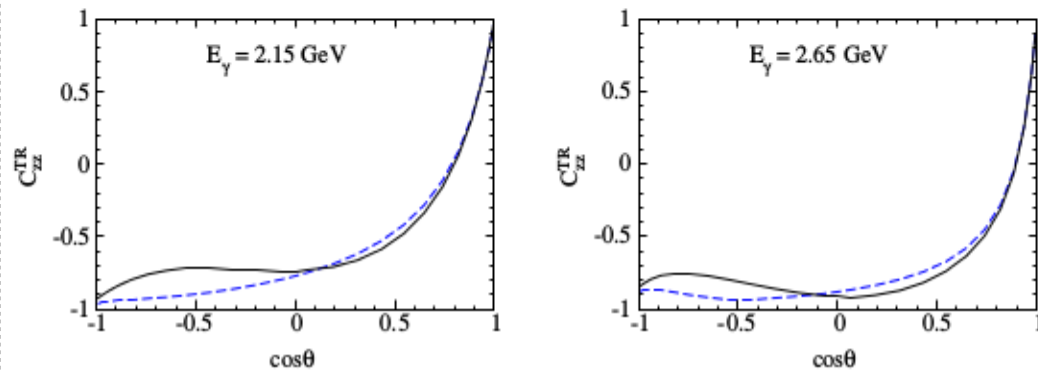
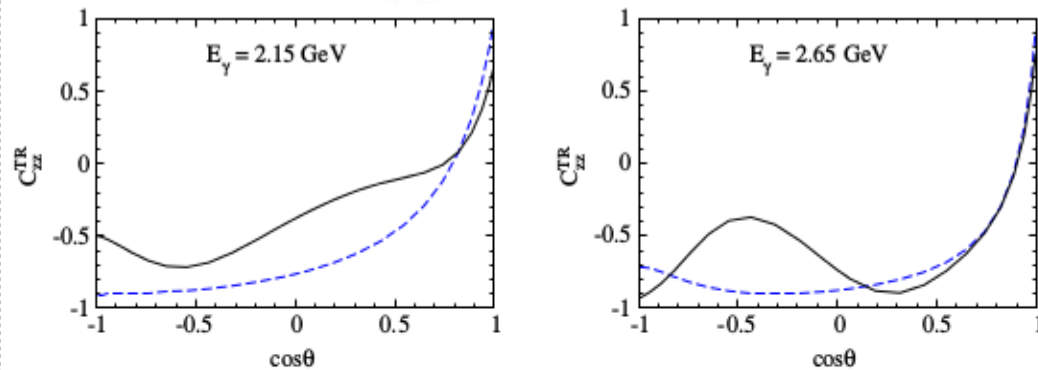
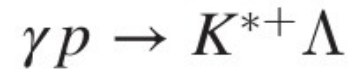
$$C_{zz}^{\text{BT}} = \frac{d\sigma(r, z; U, U) - d\sigma(r, -z; U, U)}{d\sigma(r, z; U, U) + d\sigma(r, -z; U, U)},$$

$$C_{zz}^{\text{BR}} = \frac{d\sigma(r, U; z, U) - d\sigma(r, U; -z, U)}{d\sigma(r, U; z, U) + d\sigma(r, U; -z, U)},$$

$$C_{zz}^{\text{TV}} = \frac{d\sigma(U, z; U, r) - d\sigma(U, -z; U, r)}{d\sigma(U, z; U, r) + d\sigma(U, -z; U, r)},$$

$$C_{zz}^{\text{RV}} = \frac{d\sigma(U, U; z, r) - d\sigma(U, U; -z, r)}{d\sigma(U, U; z, r) + d\sigma(U, U; -z, r)},$$

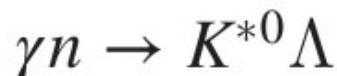
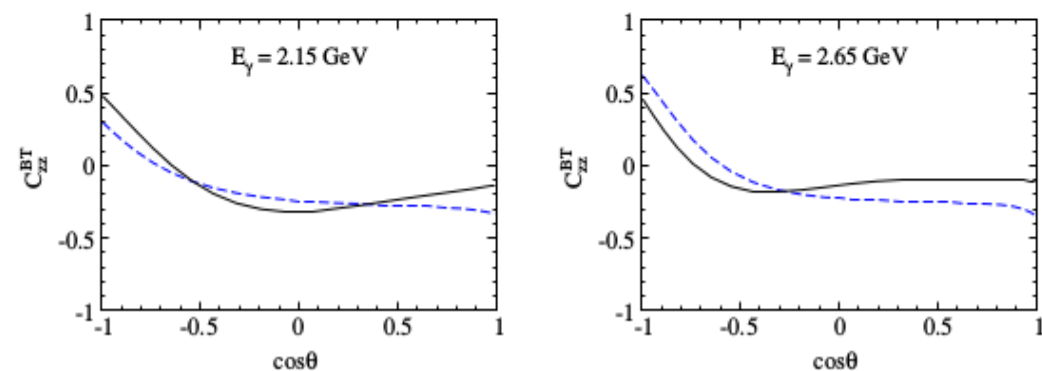
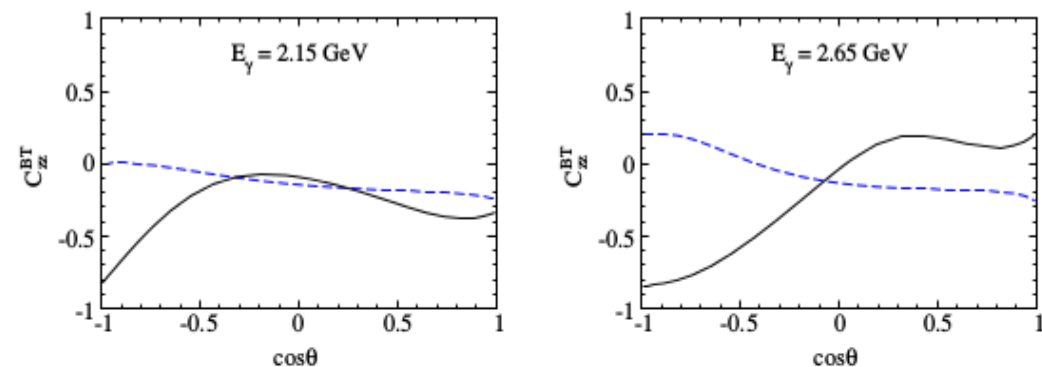
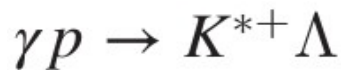
2.1. Target-Recoil Asymmetry (TR)



$$C_{zz}^{\text{TR}} = \frac{d\sigma(U, z; z, U) - d\sigma(U, z; -z, U)}{d\sigma(U, z; z, U) + d\sigma(U, z; -z, U)}$$

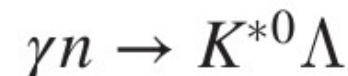
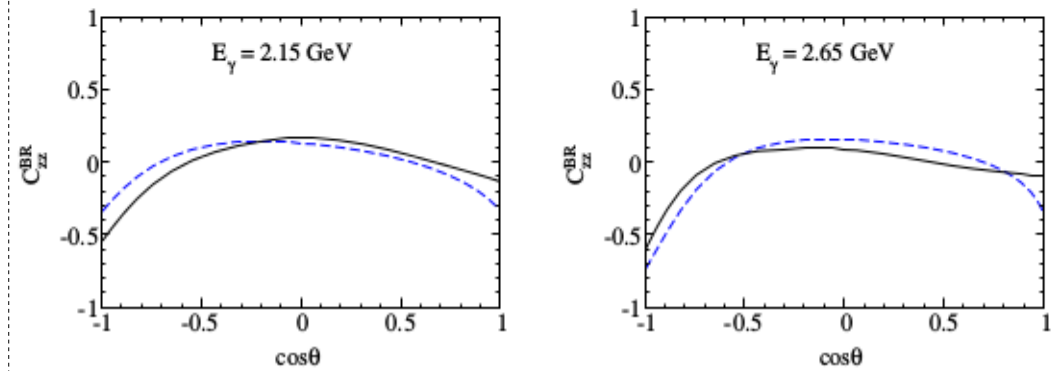
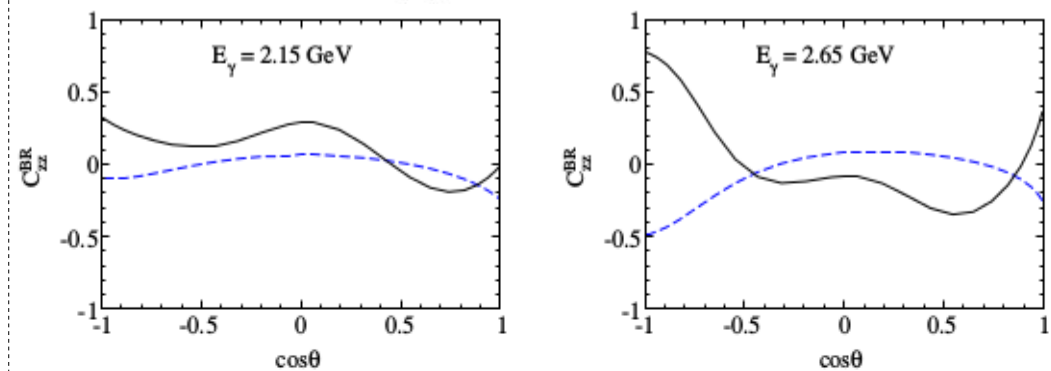
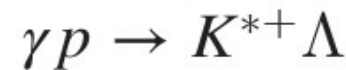
II. 3. Results : Polarization Observables

2.2. Beam-Target Asymmetry (BT)



$$C_{zz}^{BT} = \frac{d\sigma(r, z; U, U) - d\sigma(r, -z; U, U)}{d\sigma(r, z; U, U) + d\sigma(r, -z; U, U)}$$

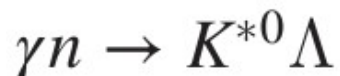
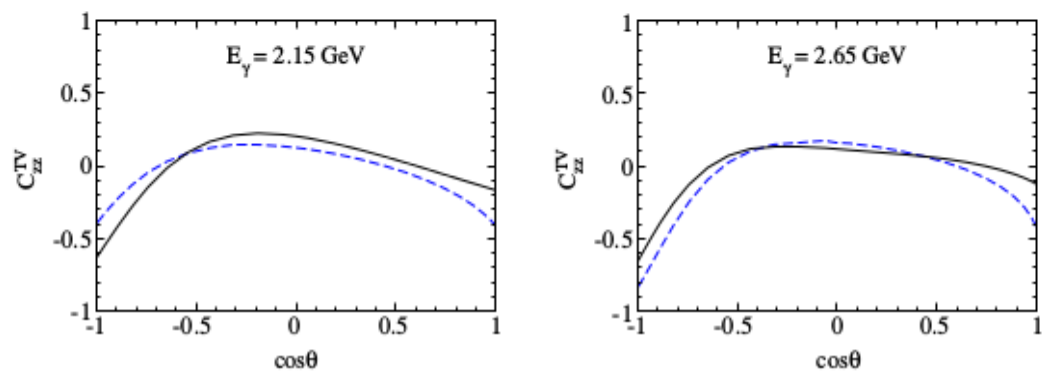
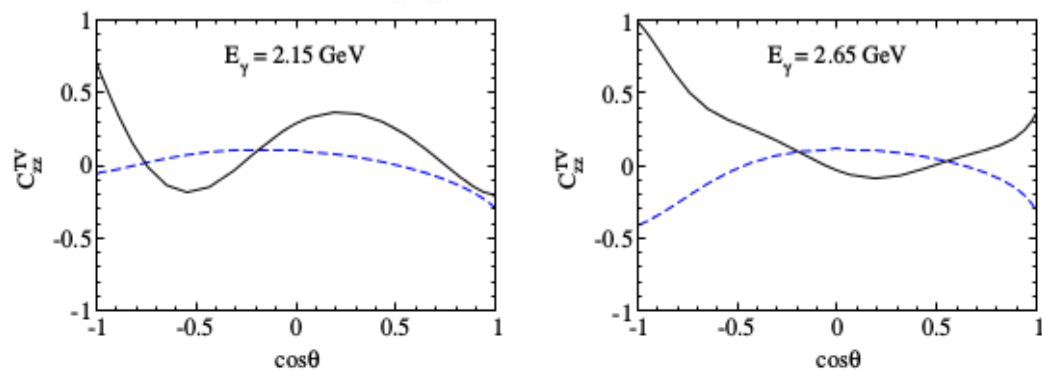
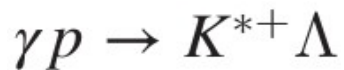
2.3. Beam-Recoil Asymmetry (BR)



$$C_{zz}^{BR} = \frac{d\sigma(r, U; z, U) - d\sigma(r, U; -z, U)}{d\sigma(r, U; z, U) + d\sigma(r, U; -z, U)}$$

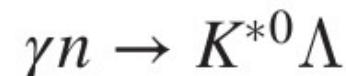
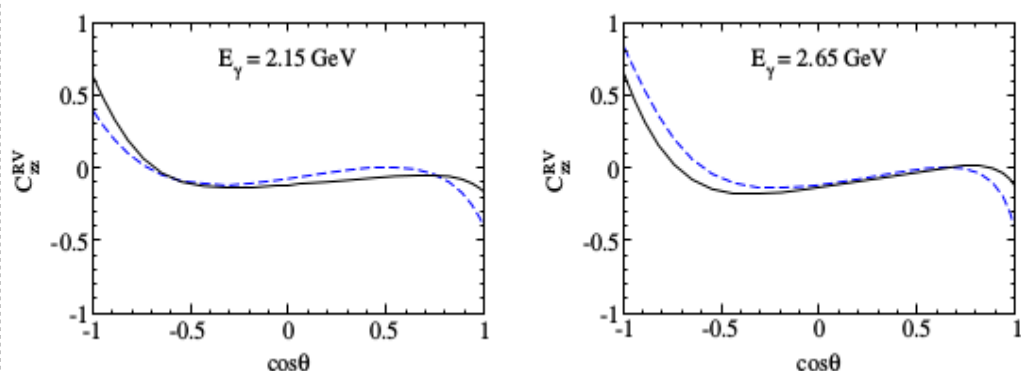
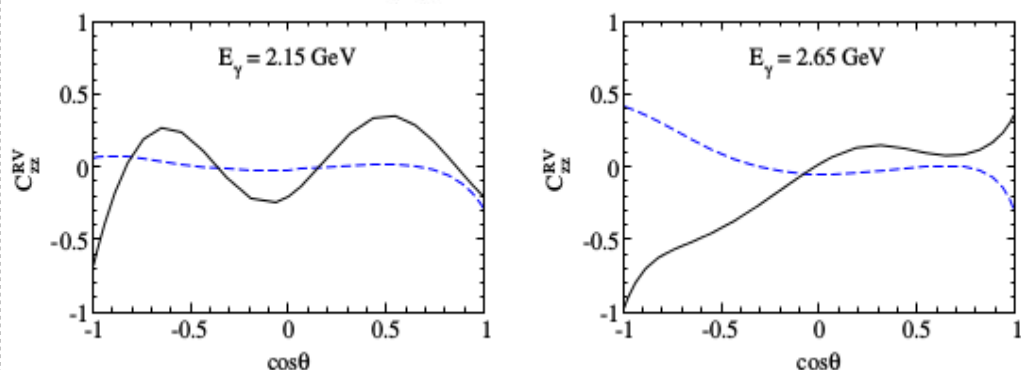
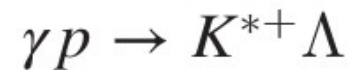
II. 3. Results : Polarization Observables

2.4. Target-V.meson Asymmetry (TV)



$$C_{zz}^{\text{TV}} = \frac{d\sigma(U, z; U, r) - d\sigma(U, -z; U, r)}{d\sigma(U, z; U, r) + d\sigma(U, -z; U, r)}$$

2.5. Recoil-V.meson Asymmetry (RV)



$$C_{zz}^{\text{RV}} = \frac{d\sigma(U, U; z, r) - d\sigma(U, U; -z, r)}{d\sigma(U, U; z, r) + d\sigma(U, U; -z, r)}$$

III. Summary

- ◇ $(\Pi p \rightarrow K^* \Lambda, \Pi p \rightarrow D^* \Lambda_c)$, within the Effective Lagrangian and Regge model.
- ◇ In Effective Lagrangian approach, we take into account the contributions of $K(D)$, $K^*(D^*)$, N , and $\Sigma(\Sigma_c)$ particles.
In Regge model, the $K^*(D^*)$, and $\Sigma(\Sigma_c)$ trajectories are considered.
The parameters are fixed by using the Quark-Gluon-String Model (QGSM).
- ◇ It turned out that the total cross section for the charm production $(\Pi p \rightarrow D^* \Lambda_c)$ is $10^4 \sim 10^6$ times smaller than that for the strange one $(\Pi p \rightarrow K^* \Lambda)$.
- ◇ $\gamma N \rightarrow K^* \Lambda(1116)$, within the tree-level Born approximation.
- ◇ In addition to K^* , K , κ , N , Λ , Σ , Σ^* contributions, we also considered nucleon resonances.
- ◇ Among them, $N(2120)$ and $N(2190)$ are important for reproducing the data for the charged K^* production.

Thank you very much